JOURNAL OF GUIDANCE, CONTROL, AND DYNAMICS
Vol. 37, No. 5, September–October 2014

Capturability of Augmented Pure Proportional Navigation Guidance Against Time-Varying Target Maneuvers

Satadal Ghosh,* Debasish Ghose,† and Soumyendu Raha‡
Indian Institute of Science, Bangalore 560012, India

DOI: 10.2514/1.G000561

This paper proposes a variation of the pure proportional navigation guidance law, called augmented pure proportional navigation, to account for target maneuvers, in a realistic nonlinear engagement geometry, and presents its capturability analysis. These results are in contrast to most work in the literature on augmented proportional navigation laws that consider a linearized geometry imposed upon the true proportional navigation guidance law. Because pure proportional navigation guidance law is closer to a realistic implementation of proportional navigation than true proportional navigation law, and any engagement process is predominantly nonlinear, the results obtained in this paper are more realistic than any available in the literature. Sufficient conditions on speed ratio, navigation gain, and augmentation parameter for capturability, and boundedness of lateral acceleration, against targets executing piecewise continuous maneuvers with time, are obtained. Further, based on a priori knowledge of the maximum maneuver capability of the target, a significant simplification of the guidance law is proposed in this paper. The proposed guidance law is also shown to require a shorter time of interception than standard pure proportional navigation and augmented proportional navigation. To remove chattering in the interceptor maneuver at the end phase of the engagement, a hybrid guidance law using augmented pure proportional navigation and pure proportional navigation is also proposed. Finally, the guaranteed capture zones of standard and augmented pure proportional navigation guidance laws against maneuvering targets are analyzed and compared in the normalized relative velocity space. It is shown that the guaranteed capture zone expands significantly when augmented pure proportional navigation is used instead of pure proportional navigation. Simulation results are given to support the theoretical findings.

I. Introduction

THE proportional navigation (PN) guidance law has been studied very extensively in the literature [1–25]. It is the most frequently used guidance philosophy due to its computational simplicity, robustness, and implementability [1]. PN was first introduced in the literature by Yuan [2] and was later analyzed by Murtaugh and Criel [3] in a linearized interceptor–target engagement geometry. Analysis of PN against a nonmaneuvering target in a nonlinear engagement framework was done for the first time by Guelman in [4] for pure proportional navigation (PPN) and in [5] for true proportional navigation (TPN). In both realizations of PN guidance, the lateral acceleration command of the interceptor is proportional to the line-of-sight (LOS) turning rate. However, in the case of PPN, the lateral acceleration is applied normal to the interceptor velocity vector, whereas in case of TPN, the lateral acceleration is applied normal to the LOS. The analysis of nonlinear equations of relative motion between the target and the interceptor in [4,5] strongly differentiated PPN and TPN in terms of capturability, as opposed to earlier linearized analysis where equivalent results were obtained for both PPN and TPN. Because obtaining a closed-form analytical solution for TPN guidance law was easier than that for PPN, in the literature TPN and its several variants have been analyzed in much detail. While Becker [6] presented the only work on the derivation of closed-form analytical solutions for PPN guidance law with a rational navigation gain, derivations of the closed-form analytical solution have been presented for TPN in [7], realistic TPN in [8], and generalization of TPN (GTPN) in [9]. Although a modification to GTPN [9] was shown to achieve an almost comparable capture zone with respect to PPN, in general, the capturability performance of PPN was found to be better than that of all forms of TPN [10]. A general study of several variants of PN guidance was done by Yang and Yang [11], whereas its extension to three-dimensional PN guidance law was analyzed by Tyan [12] with the aid of a modified polar coordinate system.

In the absence of a target maneuver in a linear interceptor guidance problem, TPN was shown to be optimal by Bryson and Ho [13], Zarchan [14], and Siouris [15]. However, the PN class of guidance laws per se does not show good performance against maneuvering targets and was found to be effective in intercepting a maneuvering target only from a restrictive set of initial geometries [16–19]. Analysis of PPN against maneuvering targets was presented by Guelman [16,17] for constant target maneuver and by Ghawghawe and Ghose [18] for a varying bounded target maneuver, whereas capturability results for TPN guidance law against an intelligently maneuvering target was presented by Ghose [19]. Garber [20] derived an optimum interceptor guidance law for maneuvering targets, which included the target lateral acceleration in the zero effort miss (ZEM) expression, which generated the idea of augmented proportional navigation (APN) guidance law, which was effectively an augmentation of the TPN guidance law. Siouris [21] presented a comparative analysis between PN and APN guidance laws. The concept of the APN guidance law in a linearized engagement framework was also presented in [1,14,15,22]. Apart from APN, several other guidance laws were also derived to account for the target lateral acceleration. Some of them had PN-based formulations [23–26], whereas others were based on optimal control [27], game theoretic problem formulation [28], differential geometry [29,30], and sliding mode control [31]. A survey of many traditional and modern guidance laws is available in [32].

Because PPN guidance law is more realistic than TPN for an aerodynamically controlled interceptor, from the point of view of implementation, augmentation of PPN guidance law to account for target maneuvers would be a more realistic proposition. However, there is no study in the literature that addresses the capturability

Received 14 February 2014; revision received 14 April 2014; accepted for publication 14 April 2014; published online 15 July 2014.

*Ph.D. Student, IISc Mathematics Initiative and Guidance, Control, and Decision Systems Laboratory, Department of Aerospace Engineering; satadal@aero.iisc.ernet.in.

†Professor, Guidance, Control and Decision Systems Laboratory, Department of Aerospace Engineering; dghose@aero.iisc.ernet.in.

‡Associate Professor, Supercomputer Education and Research Centre; raha@serc.iisc.ernet.in.

performance of the augmented PPN (APPN) guidance law in a nonlinear interceptor–target engagement framework. This was the motivation for the work in this paper, which proposes and presents an analysis of APPN and develops sufficient conditions on speed ratio, navigation gain, and augmentation parameter to ensure that all possible initial engagement geometries are included in the capture zone when applied against a target executing a piecewise continuous maneuver. It also shows that a shorter time of interception is achieved when APPN is used in the nonlinear framework. Implementation of this APPN guidance law does not require any time-to-go estimate. It is also shown that, in the presence of a priori knowledge about the target's maneuver capability, this guidance law can be reduced to a simple form of a PPN guidance law to which a bias term, the sign of which depends on that of the LOS rate, is added. Finally, the guaranteed capture zone of PPN and APPN guidance laws are analyzed in initial normalized relative velocity space and it is shown that the guaranteed capture zone expands significantly when APPN guidance law is used instead of PPN. Some results of a preliminary nature in this direction were recently presented in [33].

Organization of the paper is as follows. Section II presents the mathematical formulation of the engagement problem and introduces the APPN guidance law. In Sec. III, capturability analysis of APPN and a simplified form of APPN in the presence of knowledge of target maneuver capability and the concept of APPN + PPN guidance law are presented. Guaranteed capture zones of PPN and APPN are analyzed and compared in Sec. IV. Simulation results in support of theoretical analysis of the paper are shown in Sec. V, whereas conclusions are given in Sec. VI indicating the major contribution of the paper and possible future research work as an extension of this work.

II. Problem Formulation and Preliminary Analysis

A. Preliminaries

Consider a planar pursuit between a maneuvering target T and an APPN-guided interceptor M shown in Fig. 1. The speeds V_M and V_T of the interceptor and the target, respectively, are constants throughout the engagement. Their lateral accelerations are a_M and a_T, respectively, where throughout the pursuit a_T is assumed to be bounded and piecewise continuous in time. By piecewise continuity of a_T in time, we mean that $a_T(t)$ is defined for all time t throughout the engagement, but has simple discontinuities at a finite number of time points, that is, at those time points of discontinuity, the left- and right-hand limit of a_T are not equal [34]. The engagement is described in a relative system of coordinates centered at T and the reference is considered to be parallel to V_{T_0}, that is, the initial direction of the target velocity V_T. Therefore, from Fig. 1, $\alpha_{T_0} = 0$. The equations of motion are

$$V_R = \dot{R} = V_T \cos(\alpha_T - \theta) - V_M \cos(\alpha_M - \theta) \tag{1}$$

$$V_\theta = R\dot{\theta} = V_T \sin(\alpha_T - \theta) - V_M \sin(\alpha_M - \theta) \tag{2}$$

$$\dot{\alpha}_T = a_T/V_T \tag{3}$$

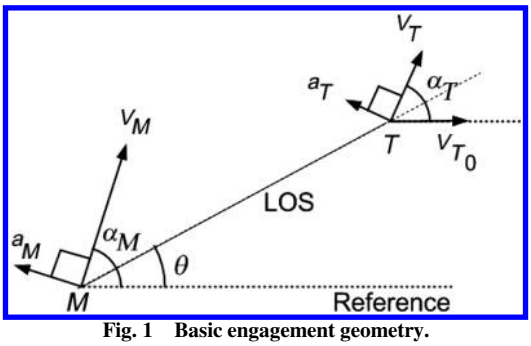

Fig. 1 Basic engagement geometry.

$$\dot{\alpha}_M = a_M/V_M \tag{4}$$

where V_R and V_θ denote the relative velocity of the target with respect to the interceptor along and normal to the LOS. Because a_T is piecewise continuous in time throughout the engagement, it is Riemann integrable [34,35]. Since $\alpha_{T_0} = 0$, integrating both sides of Eq. (3), $\alpha_T(t)$ for $t > 0$ can be obtained as

$$\alpha_T(t) = \int_0^t [a_T(\tau)/V_T]\,\mathrm{d}\tau = \int_0^t a_{n_T}(\tau)\,\mathrm{d}\tau = \hat{a}_{n_T}(t)t \tag{5}$$

where $\hat{a}_{n_T}(t) = \hat{a}_T(t)/V_T$ and

$$\hat{a}_T(t) = \left(\int_0^t a_T(\tau)\,\mathrm{d}\tau\right)/t$$

Note that $\hat{a}_T(t)$ and $\hat{a}_{n_T}(t)$, being obtained from the integration of piecewise continuous function $a_T(t)$, are continuous in time t [34,35]; $\hat{a}_T(t)$ and $\hat{a}_{n_T}(t)$ represent the average lateral acceleration and the average turn rate of the target, respectively, over time zero to t. When the target lateral acceleration is constant throughout the engagement, then $\hat{a}_T(t) = a_T$ for all time $t \in (0, t_f]$. This case was considered for PPN in [16] and for APPN in [33]. Variable target lateral acceleration was analyzed for PPN in [18].

B. Augmented Pure Proportional Navigation Guidance Law

When the missile-target engagement problem is considered in the linearized form, the PN guidance law can be expressed as one directly proportional to the ZEM and inversely proportional to the square of the time-to-go t_{go} [14]. In the presence of target maneuver, ZEM was shown to consist of an additional term corresponding to the target maneuver, and the resulting guidance law was called APN guidance law [1,14,15]. APN with effective navigation gain 3 was shown to be optimal for the problem of achieving zero miss distance subject to minimization of the integral of the square of the interceptor lateral acceleration [14] in the linearized framework. In a nonlinear framework of engagement, the APN guidance law was expressed equivalently as $a_M = N'(V_c\dot{\theta} + a_T/2)$, where N' is the effective navigation constant, V_c is the closing velocity, and a_T is the target maneuver level [14,15]. This is the augmented version of TPN, in which a term dependent on the target maneuver $(N'a_T/2)$ is added to the TPN guidance command $N'V_c\dot{\theta}$. This form of APN has been analyzed in the literature to some extent.

However, from a practical implementation point of view for an aerodynamically driven interceptor, the lateral acceleration command is applied to the interceptor in a direction normal to its velocity vector under the assumption of small angle of attack. For practical purposes, $N'V_c = NV_M$ was considered [36]. Therefore, PPN with $a_M = NV_M\dot{\theta}$ is more widely used than TPN. Therefore, augmentation of PPN guidance law would be much more realistic and relevant. Following a similar principle of the augmentation of TPN, APPN guidance law is proposed in this paper, in which an augmentation term dependent on target maneuver level is added to the PPN guidance command. The lateral acceleration command for this APPN guidance law is given by

$$a_M(t) = NV_M\dot{\theta}(t) + K_1(t)a_T(t) \tag{6}$$

where N is the navigation gain and $K_1(t)$ is the augmentation parameter represented as the coefficient associated with the target lateral acceleration $a_T(t)$ in the APPN-guided interceptor's lateral acceleration command at time t. The present work aims at the analysis of APPN in the nonlinear engagement framework. In the present study, K_1 is unknown and unlike the standard formulation of APN guidance law; here, it is not considered to remain constant throughout the engagement. Rather, it is considered to vary with time and the nature of its variation with time will be determined from the sufficient conditions of capturability.

C. Dynamics of Relative Velocity

The ratio of the interceptor speed to the target speed is defined as $\nu \triangleq V_M/V_T$. From Eqs. (4) and (6), $\dot{\alpha}_M$ can be written as

$$\dot{\alpha}_M = N\dot{\theta} + (K_1/\nu)\dot{\alpha}_T = N\dot{\theta} + K_2\dot{\alpha}_T \tag{7}$$

where $K_2 = K_1/\nu$. Since $\nu > 0$, $\text{sgn}(K_2) = \text{sgn}(K_1)$. Integrating both sides of Eq. (7),

$$\alpha_M - \alpha_{M_0} = N(\theta - \theta_0) + \int_0^t K_2(\tau)\dot{\alpha}_T(\tau)\,\mathrm{d}\tau = N(\theta - \theta_0) + \int_0^t K_2(\tau)a_{n_T}(\tau)\,\mathrm{d}\tau \Rightarrow \alpha_M = N\theta + \gamma_{n_T}(t)t + \phi_0 \tag{8}$$

where $\phi_0 = \alpha_{M_0} - N\theta_0$ and

$$\gamma_{n_T}(t)t = \int_0^t K_2(\tau)a_{n_T}(\tau)\,\mathrm{d}\tau$$

Now, substituting α_T from Eq. (5) and $\alpha_M - \theta$ from Eq. (8) in Eqs. (1) and (2), normalized $V_R(\theta, t)$ and $V_\theta(\theta, t)$ with respect to V_T are given as

$$\begin{aligned} v_R(\theta, t) &= \dot{R}/V_T = \cos\left(\int_0^t a_{n_T}(\tau)\,\mathrm{d}\tau - \theta\right) \\ &\quad - \nu\cos\left(k\theta + \int_0^t K_2(\tau)a_{n_T}(\tau)\,\mathrm{d}\tau + \phi_0\right) \\ &= \cos(\hat{a}_{n_T}(t)t - \theta) - \nu\cos(k\theta + \gamma_{n_T}(t)t + \phi_0) \end{aligned} \tag{9}$$

$$\begin{aligned} v_\theta(\theta, t) &= R\dot{\theta}/V_T = \sin\left(\int_0^t a_{n_T}(\tau)\,\mathrm{d}\tau - \theta\right) \\ &\quad - \nu\sin\left(k\theta + \int_0^t K_2(\tau)a_{n_T}(\tau)\,\mathrm{d}\tau + \phi_0\right) \\ &= \sin(\hat{a}_{n_T}(t)t - \theta) - \nu\sin(k\theta + \gamma_{n_T}(t)t + \phi_0) \end{aligned} \tag{10}$$

where $k = N - 1$. Note that $\gamma_{n_T}(t)$ and $\hat{a}_{n_T}(t)$, being continuous in time t, in Eqs. (9) and (10), $\dot{R}$ and $\dot{\theta}$ are also continuous in time t [34]. The nonlinear time-varying system of differential equations (9) and (10) defines the engagement of the interceptor and the target. In the next section, a qualitative analysis of Eqs. (9) and (10) is performed for capturability analysis of the APPN guidance law, mentioned in Eq. (6).

III. Capturability Analysis

A. Some Preliminary Results

For any given time t during the engagement, the following two results hold.

Lemma 1: For a given time t during the engagement, if $\nu > 1$ and $k\nu > 1$, then the roots of $v_R(\theta, t) = 0$ and $v_\theta(\theta, t) = 0$ alternate along the θ axis.

Lemma 2: For a given time t during the engagement, if $\nu > 1$ and $k\nu > 1$, then

$$v_R(\theta_\theta, t)\frac{\partial v_\theta(\theta_\theta, t)}{\partial\theta} > 0$$

where θ_θ is a root of $v_\theta(\theta, t) = 0$ at the given time t.

Proof (Proof of Lemma 1 and Lemma 2): Define a vector $\boldsymbol{U} \triangleq \nu e^{j(k\theta+\zeta_1)} - e^{j(\zeta_2-\theta)}$ in the complex plane, where $\zeta_1 = \gamma_{n_T}(t)t + \phi_0$ and $\zeta_2 = \hat{a}_{n_T}(t)t$. Clearly, from Eqs. (9) and (10), $v_R(\theta, t) = -Re(\boldsymbol{U})$ and $v_\theta(\theta, t) = -Im(\boldsymbol{U})$. Also, note that ζ_1 and ζ_2 are constants for a given time t. Therefore, following similar methodology as in [4,16], a strict monotonous rotation of the vector $\boldsymbol{U}$ in the complex plane can be proved, which ultimately leads to Lemmas 1 and 2. □

From Lemmas 1 and 2, the cross section of the manifolds, formed by $v_R(\theta, t)$ and $v_\theta(\theta, t)$ over the (θ, t) plane, for a given time t can be depicted in a qualitative sense, as shown in Fig. 2. The roots of $v_R(\theta, t) = 0$ and $v_\theta(\theta, t) = 0$ play a crucial role in the analysis of the equations of motion of the engagement. Now, the behavior of these roots with time t would be investigated. First, consider θ_θ to be a root of $v_\theta(\theta, t) = 0$ for a given time $t = t_\theta$. Then, from Eq. (10),

$$\hat{a}_{n_T}(t_\theta)t_\theta = [\theta_\theta + \sin^{-1}(\nu\sin(k\theta_\theta + \gamma_{n_T}(t_\theta)t_\theta + \phi_0))] \tag{11}$$

Clearly, a real t_θ exists if and only if

$$\begin{aligned} &|\nu\sin(k\theta_\theta + \gamma_{n_T}(t_\theta)t_\theta + \phi_0)| \le 1 \\ &\quad \Leftrightarrow \theta_{n_0} - (1/k)\gamma_{n_T}(t_\theta)t_\theta - (1/k)\sin^{-1}(1/\nu) \le \theta_\theta \\ &\quad \le \theta_{n_0} - (1/k)\gamma_{n_T}(t_\theta)t_\theta + (1/k)\sin^{-1}(1/\nu) \end{aligned} \tag{12}$$

Here, $\theta_{n_0} = -(\phi_0 + n\pi)/k$; $n = 0, \pm1, \pm2, \ldots$. Next, consider that θ_R is a root of $v_R(\theta, t) = 0$ for $t = t_R$. Then, from Eq. (9),

$$\hat{a}_{n_T}(t_R)t_R = [\theta_R + \cos^{-1}(\nu\cos(k\theta_R + \gamma_{n_T}(t_R)t_R + \phi_0))] \tag{13}$$

Clearly, here a real t_R exists if and only if

$$\begin{aligned} &|\nu\cos(k\theta_R + \gamma_{n_T}(t_R)t_R + \phi_0)| \le 1 \\ &\quad \Leftrightarrow \theta_{n_0} - (1/k)\gamma_{n_T}(t_R)t_R - (1/k)\sin^{-1}(1/\nu) + \pi/(2k) \le \theta_R \\ &\quad \le \theta_{n_0} - (1/k)\gamma_{n_T}(t_R)t_R + (1/k)\sin^{-1}(1/\nu) + \pi/(2k) \end{aligned} \tag{14}$$

where $n = m + 1 = 0, \pm1, \pm2, \ldots$ and θ_{n_0} is as defined earlier. For different values of n, the inequalities (12) and (14) produce different intervals in the θ axis inside which the roots of v_θ and v_R, respectively, lie at time t during the pursuit. Therefore, inequalities (12) and (14)

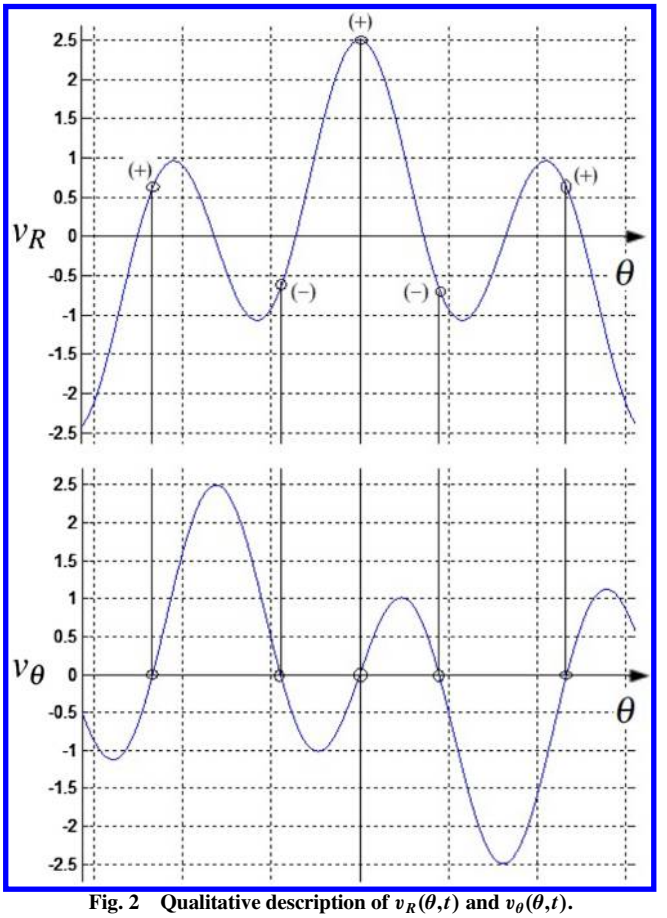

Fig. 2 Qualitative description of $v_R(\theta,t)$ and $v_\theta(\theta,t)$.

determine that, at any time t during the engagement, there exist two classes of sectors in the polar plane of relative pursuit, which are denoted as $S_\theta(t)$ and $S_R(t)$, as defined next and shown in Fig. 3:

$$S_\theta(t) \triangleq [\theta_{n_0} - (1/k)\gamma_{n_T}(t)t - (1/k)\sin^{-1}(1/\nu), \theta_{n_0} - (1/k)\gamma_{n_T}(t)t + (1/k)\sin^{-1}(1/\nu)] \quad (15)$$

$$S_R(t) \triangleq [\theta_{n_0} - (1/k)\gamma_{n_T}(t)t - (1/k)\sin^{-1}(1/\nu) + \pi/(2k), \theta_{n_0} - (1/k)\gamma_{n_T}(t)t + (1/k)\sin^{-1}(1/\nu) + \pi/(2k)] \quad (16)$$

Note that by Eqs. (15) and (16) the sectors $S_\theta(t)$ and $S_R(t)$ in the polar plane are well defined for all time t during the engagement. Clearly, $\theta_\theta(t) \in S_\theta(t)$ and $\theta_R(t) \in S_R(t)$. Here, $S_\theta(t)$ and $S_R(t)$ are dependent on time t and the maneuver profile $a_T(t)$ of the target, whereas in [16,18], these sectors were invariant with time or target maneuvers. Hence, this is the point of departure of the analysis presented in this paper from that in [16,18].

From Eqs. (15) and (16), the following observations can be made for any time t during the engagement.

Observation 1: The locations of the sectors $S_\theta(t)$ and $S_R(t)$ depend on initial conditions θ_{n_0}, navigation gain N, the target maneuver profile $a_T(t)$, and time t in the form that $S_\theta(t)$ sectors are centered around $\theta_{n_0} - \gamma_{n_T}(t)t/k$ and the $S_R(t)$ sectors are centered around $\theta_{n_0} - \gamma_{n_T}(t)t/k + \pi/2k$, for various integer values of n.

Observation 2: The angular spread ω of each sector depends only on the navigation gain N and speed ratio υ and is given by $\omega = (2/k)\sin^{-1}(1/\nu)$.

Observation 3: The angular separation between the centerline of two adjacent sectors is given as $\delta = \pi/2k$.

Observation 4: These sectors do not overlap if $\nu > \sqrt{2}$.

From Eqs. (15) and (16) and Observation 1, by Leibnitz's rule of differentiation [37], these sectors rotate in the polar plane of relative pursuit at an angular rate of $-K_2(t)a_{n_T}(t)/k$ at time t. Thus, only Observation 1 is different from [16,18], whereas Observations 2–4 are same as in [16,18]. For the sake of brevity, only $K_2 a_{n_T}(t)$ will be mentioned instead of $K_2(t)a_{n_T}(t)$ throughout the paper. In all subsequent analysis $\nu = V_M/V_T > \sqrt{2}$ is considered, which ensures that, at any time t, sectors $S_\theta(t)$ and $S_R(t)$ are disjoint to each other and they alternate in sequence under an additional condition $k\nu > 1$. Then, at any time t, the following eight different classes of sectors, which rotate at an angular rate $-K_2 a_{n_T}(t)/k$ in the polar plane of relative pursuit of the interceptor M with respect to the target T located at the center of the polar plane, as shown in Fig. 3, can be defined:

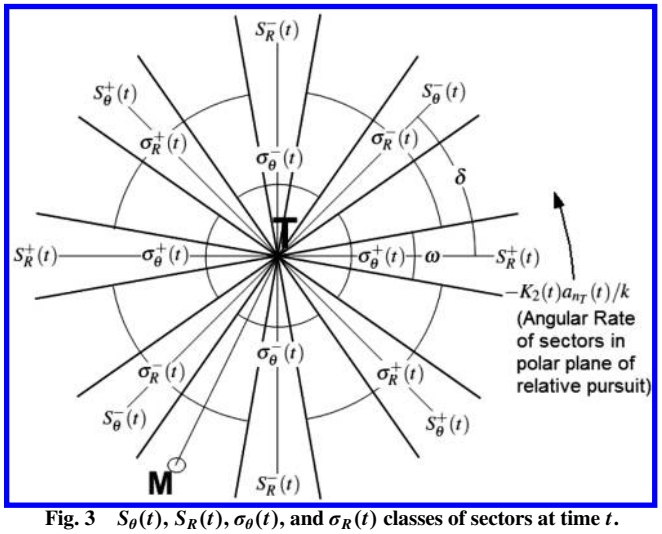

Fig. 3 $S_\theta(t)$, $S_R(t)$, $\sigma_\theta(t)$, and $\sigma_R(t)$ classes of sectors at time t.

$$S_\theta^+(t) = \{\theta : \theta \in S_\theta(t), v_R(\theta,t) > 0\}; \quad S_\theta^-(t) = \{\theta : \theta \in S_\theta(t), v_R(\theta,t) < 0\}$$
$$S_R^+(t) = \{\theta : \theta \in S_R(t), v_\theta(\theta,t) > 0\}; \quad S_R^-(t) = \{\theta : \theta \in S_R(t), v_\theta(\theta,t) < 0\}$$
$$\sigma_\theta^+(t) = \{\theta : \theta \in S_\theta^c(t), v_\theta(\theta,t) > 0\}; \quad \sigma_\theta^-(t) = \{\theta : \theta \in S_\theta^c(t), v_\theta(\theta,t) < 0\}$$
$$\sigma_R^+(t) = \{\theta : \theta \in S_R^c(t), v_R(\theta,t) > 0\}; \quad \sigma_R^-(t) = \{\theta : \theta \in S_R^c(t), v_R(\theta,t) < 0\} \quad (17)$$

where the superscript c denotes the complement of a set. The sectors defined earlier and shown in Figs. 3 and 4 are necessary for the analysis of the relative trajectory of M in the polar plane, which would be interchangeably termed as the trajectory of M in the polar plane in the subsequent study. At time t, the collision course is described as the collection of θ such that $v_R(\theta, t) < 0$; $v_\theta(\theta, t) = 0$, whereas the inverse collision course is described as the collection of θ such that $v_R(\theta, t) > 0$; $v_\theta(\theta, t) = 0$. Therefore, from Eq. (17) note that $S_\theta^-(t)$ and $S_\theta^+(t)$ represent the neighborhoods of the collision course and the inverse collision course, respectively, at time t.

B. Capturability Analysis for Points Exterior to $S_\theta^+(t)$

In [16], it was shown that a PN-guided interceptor can intercept a target maneuvering with a constant lateral acceleration if the initial interceptor orientation with respect to the target is exterior to the sector S_θ^+. However, as noted in Sec. III.A., unlike the PN guidance scenario, in the case of APPN guidance law, the sectors in the polar plane are not stationary throughout the engagement period and rotate in the polar plane at an angular rate of $-K_2 a_{n_T}(t)/k$ at time t. Furthermore, the $S_\theta(t)$ sectors are centered around $\theta_{n_0} - \gamma_{n_T}(t)t/k$ and the $S_R(t)$ sectors are centered around $\theta_{n_0} - \gamma_{n_T}(t)t/k + \pi/2k$ for various integer values of n at time t. In this section, the focus will be on determining the sign of the augmentation parameter $K_1(t)$ such that this rotation of the sectors in the polar plane can be used favorably by the interceptor when the engagement starts from an initial condition outside the neighborhood of the inverse collision course.

Lemma 3: Consider an interceptor pursuing a target, executing a piecewise continuous maneuver $a_T(t)$, with $\nu > \sqrt{2}$ and $k\nu > 1$. If the interceptor lies in the sector $\sigma_\theta^-(t)$ ($\sigma_\theta^+(t)$) at some time $t = t_1$ during the engagement, then if the augmentation parameter $K_1(t)$ is such that $\mathrm{sgn}(K_1(t)) = -\mathrm{sgn}(a_T(t))$ $(= \mathrm{sgn}(a_T(t)))$, that is, $\mathrm{sgn}(K_1(t)) = \mathrm{sgn}(a_T\theta(t))$, for all $t \geq t_1$, then, in the polar plane, M will enter the sector $S_\theta^-(t)$ at some finite time $t > t_1$.

Proof. See Appendix for detailed proof. □

From Lemma 3, it is evident that, at any time t, if the interceptor M is neither in the neighborhood of collision course nor in the neighborhood of inverse collision course in the polar plane, then, if the sign of the augmentation parameter is maintained depending on the signs of target lateral acceleration and LOS rate, as indicated in the Lemma, then APPN ensures that the interceptor enters the neighborhood of collision course at some finite time.

From ([16] Theorem 1) and ([18] Theorem 1), it is evident that, if the sectors do not rotate in the polar plane, then, in the polar plane, once M is in the S_θ^- sector, M remains inside S_θ^- until the origin T is reached. However, when the sectors rotate in the polar plane, then under some sufficient conditions, derived in the following Lemma, it can be ensured that, once M is in $S_\theta^-(t)$ at time $t = t_1$, M remains in $S_\theta^-(t)$ for all time $t \geq t_1$.

Lemma 4: Consider an interceptor, pursuing a target executing a piecewise continuous maneuver $a_T(t)$, with $\nu > \sqrt{2}$ and $k\nu > 1$.

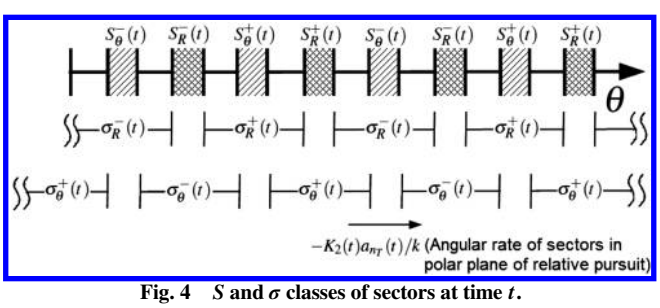

Fig. 4 S and σ classes of sectors at time t.

If the interceptor is in the sector $S_\theta^-(t)$ at some time $t = t_1$ during the engagement, then, if the augmentation parameter $K_1(t)$ is such that $\text{sgn}(K_1(t)) = \text{sgn}(a_T\dot{\theta}(t))$ for all $t \geq t_1$ then, in the polar plane, M will remain inside the sector $S_\theta^-(t)$ for all time $t > t_1$ until interception.

Proof: See Appendix for detailed proof. □

Thus, Lemma 4 gives a sufficient condition on the sign of the augmentation parameter, dependent on the signs of target lateral acceleration and LOS rate, which ensures that, once the interceptor M reaches the neighborhood of the collision course at some time t, it remains in the neighborhood of collision course for all subsequent time until interception. The preceding results lead to the following theorem.

Theorem 1: Consider an ideal interceptor, guided by the APPN guidance law with navigation gain N, interceptor speed V_M, and augmentation parameter $K_1(t)$, pursuing a maneuvering target with speed V_T and a piecewise continuous maneuver $a_T(t)$ such that 1) $\nu = V_M/V_T > \sqrt{2}$, 2) $N > 1 + 1/\nu$, and 3) $\text{sgn}(K_1(t)) = \text{sgn}(a_T\dot{\theta}(t))$, where $\dot{\theta}(t)$ is the LOS rate at time t, then the interceptor reaches the target from any initial state $M_0(r_0, \theta_0)$ exterior to $S_\theta^+(t_0)$ in the polar plane. Moreover, M reaches the origin T of the polar plane in the interior of $S_\theta^-(t)$ sector at some finite time $t > t_0$.

Proof: From Lemmas 1 and 2 and their subsequent observations in Sec. III.A, when the conditions $\nu > \sqrt{2}$ and $N > 1 + 1/\nu$ hold true, then the sectors $S_\theta(t)$ and $S_R(t)$ remain alternate to each other and they do not overlap at any time t. By Lemma 3, if the initial state of M at time $t = t_0$ is inside the $\sigma_\theta(t_0)$ sector in the polar plane, then, if the augmentation parameter $K_1(t)$ is such that $\text{sgn}(K_1(t)) = \text{sgn}(a_T\dot{\theta}(t))$, M enters the $S_\theta^-(t)$ sector at some finite time $t > t_0$. Again, from Lemma 4, if M is in the sector $S_\theta^-(t_1)$ in the polar plane at time $t = t_1$, then, if the augmentation parameter $K_1(t)$ is such that $\text{sgn}(K_1(t)) = \text{sgn}(a_T\dot{\theta}(t))$ for all $t \geq t_1$, M remains inside the sector $S_\theta^-(t)$ for all subsequent time during the pursuit until the interceptor hits the target in some finite time. Since $v_\theta(\theta, t) = 0$ isocurve always lies in the $S_\theta(t)$ sector and $S_\theta^-(t) \subset \sigma_R^-(t)$, M reaches the origin T of the polar plane along some angle $\theta \in S_\theta^-(t)$ at some finite time t on the $v_\theta(\theta, t) = 0$ isocurve. □

If $a_T(t) = 0$ for all time t during the engagement, that is, if the target is nonmaneuvering, the APPN guidance law becomes simply PPN. In that case, sectors in the polar plane of relative pursuit are time independent and the S_θ^+ sector represents only a particular angle. Conditions on navigation gain N, mentioned in Theorem 1, ensure that the capturability of the APPN guidance law remains the same as that of the PPN, demonstrated in ([4] Theorem 2). Also, if the augmentation parameter $K_1(t) = 0$ in Eq. (6) in the presence of nonzero $a_T(t)$, that is, maneuvering target, for all time t during the engagement, the APPN guidance law becomes simply PPN. It has been shown in [16,18] that, when the initial condition of M in the polar plane is exterior to the S_θ^+ sector, a PPN-guided interceptor intercepts a target maneuvering with a constant and a piecewise continuous lateral acceleration, respectively, under the conditions 1 and 2, mentioned in Theorem 1 in this paper. However, the APPN guidance law, with the additional condition 3 in Theorem 1, ensures higher magnitude of relative angular rate $\dot{\theta}_{\text{rel}}(t)$ of M with respect to the sectors in the polar plane at any $(r(t), \theta(t))$ in the polar plane at time t, and thus makes M approach the $S_\theta^-(t)$ sector and also the $v_\theta(\theta, t) = 0$ isocurve faster.

C. Capturability Analysis for $M_0(r_0,\theta_0) \in S_\theta^+(t_0)$

In ([16] Theorem 2) and ([18] Theorem 2 and Corollary 2), a sufficient condition on $\dot{\theta}_0$ was obtained for $\theta_0 \in S_\theta^+$, such that M can come out of the S_θ^+ sector and eventually reach the origin T of the polar plane. The following analysis is similar to that in [16,18], but the main difference is that the present analysis aims at determining the augmentation parameter $K_1(t)$, such that the sufficient condition on $\dot{\theta}_0$ in [16,18] can be relaxed when the engagement starts from an initial condition in the neighborhood of the inverse collision course. Differentiating both sides of Eq. (10) and multiplying them by V_T, we obtain

$$\dot{V}_\theta(\theta, t) = \dot{R}\,\dot{\theta} + R\ddot{\theta} = V_T[a_{n_T}(t) - \dot{\theta}]\cos\left(\int_0^t a_{n_T}(\tau)\,\mathrm{d}\tau - \theta\right) - V_M[k\dot{\theta} + K_2 a_{n_T}(t)]\cos\left(k\theta + \int_0^t K_2 a_{n_T}(\tau)\,\mathrm{d}\tau + \phi_0\right)$$

$$\Rightarrow R\ddot{\theta} = V_S(t)\dot{\theta} + a_{n_T}(t)[V_T\cos(\hat{a}_{n_T}(t)t - \theta) - K_2(t)V_M\cos(k\theta + \gamma_{n_T}(t)t + \phi_0)] \tag{18}$$

where

$$V_S(t) \triangleq -(N-2)V_M\cos(k\theta + \gamma_{n_T}(t)t + \phi_0) - 2V_T\cos(\hat{a}_{n_T}(t)t - \theta) \tag{19}$$

Since $S_\theta^+(t) \subset \sigma_R^+(t)$, as shown in Fig. 4, $v_R(\theta, t) > 0$in $S_\theta^+(t)$. From Eq. (9), the necessary condition for $v_R(\theta, t) > 0$ is $\cos(k\theta + \gamma_{n_T}(t)t + \phi_0) < 0$, since $\nu > \sqrt{2}$, otherwise $v_R(\theta, t)$ would be negative in $\sigma_R^+(t)$, which is infeasible by definition. Again, from inequality (12), $|\sin(k\theta + \gamma_{n_T}(t)t + \phi_0)| \leq 1/\nu$ for $\theta(t) \in S_\theta^+(t)$. Hence,

$$\cos(k\theta + \gamma_{n_T}(t)t + \phi_0) \leq -\sqrt{\nu^2 - 1}/\nu \tag{20}$$

Lemma 5: For any time t during the engagement, if $\theta(t) \in S_\theta^+(t)$ and $N > 2$, then $V_S(t) \geq V_e = V_T[(N-2)\sqrt{\nu^2 - 1} - 2]$.

Proof: Since $-1 \leq \cos(\hat{a}_{n_T}(t)t - \theta) \leq 1$, from Eqs. (19) and (20), the result is straightforward. □

Note from Eq. (19) that $V_S(t)$ is continuous in t, and from Lemma 5 note that V_e, the lower bound of $V_S(t)$ for $\theta(t) \in S_\theta^+(t)$, is independent of time.

Lemma 6: If $\theta = \theta(t)$ is a solution of Eqs. (9) and (10) such that $\dot{\theta}(t) > \dot{\theta}_1(t)$ $(< \dot{\theta}_1(t))$ for all time t, where $\dot{\theta}_1$ is defined as $V_S(t)\dot{\theta}_1 = a_{n_T}(t)[K_2(t)V_M\cos(k\theta_1 + \gamma_{n_T}(t)t + \phi_0) - V_T\cos(\hat{a}_{n_T}(t)t - \theta_1)]$, then, if 1) $V_S(t) > 0$ for all t, $\dot{\theta}$ is an increasing (decreasing) function of t for all time t; and if 2) $V_S(t) < 0$ for all t, $\dot{\theta}$ is an decreasing (increasing) function of t for all time t.

Proof: See Appendix for detailed proof. □

The results in Lemmas 5 and 6 lead to the following theorem.

Theorem 2: Consider an ideal interceptor, guided by the APPN guidance law with navigation gain N, interceptor speed V_M, and augmentation parameter $K_1(t)$, pursuing a maneuvering target with speed V_T and a piecewise continuous maneuver $a_T(t)$ such that, 1) $\nu > \sqrt{2}$, 2) $N > 2 + 2/\sqrt{\nu^2 - 1} > 1 + 1/\nu$, 3) $\text{sgn}(K_1) = \text{sgn}(a_T\dot{\theta}(t))$, and 4) $|K_1| > 1/\sqrt{1 - 1/\nu^2}$, where $\dot{\theta}(t)$ is the LOS rate at time t, then the interceptor reaches the target in some finite time $t > t_0$ from an initial state $M_0(r_0, \theta_0) \in S_\theta^+(t_0)$ in the polar plane for any value of $\dot{\theta}_0$.

Proof: See Appendix for detailed proof. □

Thus, Theorem 2 relaxes the conditions on initial LOS rate $\dot{\theta}_0$ in the neighborhood of inverse collision course $S_\theta^+(t_0)$and derives sufficient conditions on the navigation gain and augmentation parameter, such that, if the engagement starts from an initial condition in the neighborhood of the inverse collision course, M can leave the neighborhood at some finite time $t > t_0$ and finally reach the origin T in the polar plane in some finite time. This relaxation of condition on $\dot{\theta}_0$ along with the notion of faster time of interception justifies the use of the augmentation parameter $K_1(t)$ in the APPN guidance law. Also, if $a_T(t) = 0$, that is, if the target is nonmaneuvering, $\dot{\theta}_1(t) = 0$ for all time t in inequalities (A8) and (A9). Therefore, guided by the APPN guidance law, which becomes simply PPN when $a_T(t) = 0$, an interceptor can intercept a nonmaneuvering target from any initial geometry, except when $\dot{\theta}_0 = 0$ with $v_{R_0} > 0$, under Conditions 1 and 2 in Theorem 2.

D. Conditions on Interceptor Lateral Acceleration

In the implementation of a guidance law, an important factor is the limitation on the interceptor lateral acceleration capability. From Eq. (6), the lateral acceleration command in the APPN guidance law has one component proportional to the LOS rate $\dot{\theta}$ and another

component proportional to the target lateral acceleration a_T, which is considered here to be bounded and piecewise continuous in time. Therefore, to ensure a finite demand of interceptor lateral acceleration, $\dot{\theta}$ should not become unbounded. It is evident that, if the conditions on N, ν, and $K_1(t)$, mentioned in Theorems 1 and 2, are satisfied for all time t during the engagement, then from any initial state, the APPN-guided interceptor can intercept a target maneuvering with a piecewise continuous lateral acceleration at some finite time t and in the polar plane of relative pursuit, interception occurs within the $S_\theta^-(t)$ sector, the neighborhood of collision course. The following result determines a sufficient condition on $K_1(t)$ to achieve finiteness of the lateral acceleration demand in the $S_\theta^-(t)$ sector at any given time t.

Theorem 3: Consider an ideal interceptor, guided by the APPN guidance law with navigation gain N, interceptor speed V_M, and augmentation parameter $K_1(t)$, pursuing a maneuvering target with speed V_T and piecewise continuous maneuver $a_T(t)$, such that $\nu > \sqrt{2}$ and $N > 2 + 2/\sqrt{\nu^2 - 1} > 1 + 1/\nu$. If the interceptor lies in the sector $S_\theta^-(t)$, in the polar plane, at some time $t = t_1$ during the engagement then, if $K_1(t)$ is such that 1) $\text{sgn}(K_1(t)) = \text{sgn}(a_T\dot{\theta}(t))$ and 2) $|K_1(t)| > 1/\sqrt{1 - 1/\nu^2}$, where $\dot{\theta}(t)$ is the LOS rate at time t, then the interceptor intercepts the target at some finite time $t = t_2 > t_1$ in a way that, if $|\dot{\theta}(t)| > 0$ for any $t \in [t_1, t_2)$, then subsequently $|\dot{\theta}(t)|$ decreases until $|\dot{\theta}(t)| = 0$.

Proof: See Appendix for detailed proof. □

Theorem 3 gives sufficient conditions on the navigation gain and augmentation parameter to ensure that $|\dot{\theta}(t)|$ decreases to zero from any nonzero value in the neighborhood of the collision course at the endgame of the engagement, which in turn helps in achieving finite demand of interceptor lateral acceleration. In continuous time systems, once $|\dot{\theta}(t)| = 0$ is achieved, the magnitude of the oscillation of $\dot{\theta}$ remains arbitrarily close to zero by Theorem 3, which, from Eq. (6), implies that ideally $a_M(t)$ also oscillates about zero as $\dot{\theta}$ reaches zero once. However, in practical implementation, one needs to deal with discrete time systems, in which the magnitude of chattering of $\dot{\theta}$ might depend on the sampling interval in the form that a higher sampling interval could imply larger deviation of M from the $v_\theta(\theta, t) = 0$ isocurve in the polar plane on the subsequent sampling instant. This ultimately causes a chattering in $a_M(t)$, as can be seen from Eq. (6). From Theorem 3, the following result for constant target lateral acceleration can be obtained in a straightforward manner.

Corollary 1: Consider an ideal interceptor, guided by APPN guidance law with navigation gain N, interceptor speed V_M, and augmentation parameter $K_1(t)$, pursuing a maneuvering target with speed V_T and constant maneuver a_T such that $\nu > \sqrt{2}$ and $N > 2 + 2/\sqrt{\nu^2 - 1} > 1 + 1/\nu$. If the interceptor lies in the sector $S_\theta^-(t)$, in the polar plane, at some time $t = t_1$ during the engagement, then, if K_1 is such that 1) $\text{sgn}(K_1) = \text{sgn}(a_T\dot{\theta}(t))$ and 2) $|K_1| > 1/\sqrt{1 - 1/\nu^2}$, where $\dot{\theta}(t)$ is the LOS rate at time t, then the interceptor intercepts the target in some finite time $t = t_2 > t_1$ in a way that, if $|\dot{\theta}(t)| > 0$ for any $t \in [t_1, t_2)$, then subsequently $|\dot{\theta}(t)|$ decreases until $|\dot{\theta}(t)| = 0$.

For constant target maneuver and constant magnitude of augmentation parameter $K_1(t)$, Corollary 1 implies that, if all the conditions of Corollary 1 hold good and if $|a_M(t)| > \hat{a}_M = |K_1 a_T|$ for any $t \in [t_1, t_2)$, then subsequently $|a_M(t)|$ would decrease until $|a_M(t)| = \hat{a}_M$, and once $|a_M(t)|$ reaches $\hat{a}_M$, the lateral acceleration of the interceptor $a_M(t)$ remains arbitrarily close to the twin surface $a_M = \pm\hat{a}_M$ until interception. However, as discussed earlier, in practical implementation with discrete time systems, a chattering of $\dot{\theta}$ about $\dot{\theta} = 0$ is observed, which also leads to a chattering in $a_M(t)$ about the twin surface $a_M = \pm\hat{a}_M$.

E. Significant Simplification of APPN

From the results obtained earlier, a very important result on the simplification of the APPN guidance law would be obtained now, which establishes that, if the target's maneuver capability is known a priori, then the PPN guidance law, to which a bias term dependent on target maneuver capability and sign of LOS rate is added, would achieve successful interception of the piecewise continuously maneuvering target with finite lateral acceleration of the interceptor at the endgame of the engagement.

Corollary 2: Consider an ideal interceptor pursuing a target with speed V_T and piecewise continuous maneuver $a_T(t)$, bounded as $-a_{T_{\max}} \le a_T(t) \le a_{T_{\max}}$, such that $\nu > \sqrt{2}$. If the interceptor is guided by a simplified form of APPN guidance law, given as $a_M = C_1\text{sgn}(\dot{\theta})$, where $C_1 = NV_M|\dot{\theta}| + C_2$ is a time-varying parameter with navigation gain $N > 2 + 2/\sqrt{\nu^2 - 1} > 1 + 1/\nu$ and the bias term $C_2 = a_{T_{\max}}\sqrt{1 - 1/\nu^2}$, then, from any initial engagement geometry, the interceptor can reach the target in finite time with finite lateral acceleration at the endgame of the engagement.

Proof: See Appendix for detailed proof. □

The simplified form of APPN guidance law, given in Corollary 2, is essentially a combination of the standard PPN and a bias term, magnitude and sign of which depend on maximum target maneuver capability (apart from speed ratio), and the sign of LOS rate, respectively. Apart from measuring LOS rate at every instant, the implementation of this form of APPN requires only the a priori knowledge of target maneuver capability instead of estimating the target lateral acceleration at every instant. It is interesting to note that, on the availability of a priori knowledge about the target's maneuver capability, the simplified formulation of APPN Eq. (A16) is structurally similar to the guidance law derived in [23].

F. APPN + PPN Guidance Law

From the previous discussion, it is evident that APPN has two major advantages. First, it leads to a faster approach of M toward the $S_\theta^-(t)$ sector and the $v_\theta(\theta, t) = 0$ isocurve in the polar plane, as explained in the discussion subsequent to Theorem 1 in Sec. III.B. Second, it relaxes the condition on $\dot{\theta}_0$ in $S_\theta^+(t_0)$ and ensures interception of a maneuvering target from any initial condition, which is evident from Theorems 1 and 2. This would be reflected in the results on the guaranteed capture zone of PPN and APPN in initial normalized relative velocity space [(v_{θ_0}, v_{R_0}) plane] from Theorems 4 and 5 in the next section. Further, in the presence of a priori knowledge about target maneuver, the simplified realization of APPN as PPN with a bias term added to it has another advantage, in that there is no need to estimate a_T at every instant and feed that estimate to the guidance command, thus making it possible to avoid a significantly difficult task of estimating a_T.

However, a drawback of APPN could also be noted from the subsequent discussion of Theorem 3 and Corollary 1 in Sec. III.D. In practical implementation, there would be chattering and frequent instantaneous jumps in the lateral acceleration of the interceptor at the end phase of the engagement, when M is very close to the $v_\theta(\theta, t) = 0$ isocurve in the $S_\theta^-(t)$ sector. It puts a strain on the control surfaces. Therefore, practically, APPN may not be useful at the terminal phase of the engagement. As a remedy, the notion of APPN + PPN is introduced, in which the augmentation parameter of APPN is considered to be gradually driven to zero as M enters the $S_\theta^-(t)$ sector in the polar plane at some time t, which implies the guidance law of the interceptor is gradually changed from APPN to PPN, hence the name APPN + PPN. This gradual change can be done in many ways. A simple way would be to change the magnitude of the augmentation parameter to zero instantaneously when $|\dot{\theta}(t)|$ is smaller than a threshold that is sufficiently close to zero. Simulation results for this are shown in Sec. V.C.

Note that this remedy ensures a faster approach of M toward the $S_\theta^-(t)$ sector from any initial engagement geometry and also, at the same time, a smooth and bounded [ensured by ([16] Theorem 3) and ([18] Theorem 3)] lateral acceleration profile of the interceptor throughout the engagement, including its end phase.

IV. Analysis of Guaranteed Capture Zone in the Relative Velocity Space

In this section, first, the sectors in the target-centered coordinate system would be represented in the interceptor-centered LOS-fixed coordinate system and then some results on the guaranteed capture

zone would be derived for both PPN and APPN. Finally, the superiority of APPN over PPN against maneuvering targets would be indicated in terms of guaranteed capture zone.

A. Representation of Sectors in the Interceptor-Centered LOS Referenced Frame

From Eq. (8),

$$\theta = (\alpha - \gamma_{n_T}(t)t - \phi_0)/k \Rightarrow \theta_\theta = (\alpha_\theta - \gamma_{n_T}(t_\theta)t_\theta - \phi_0)/k \quad (21)$$

where $\alpha = \alpha_M - \theta$ and θ_θ is a root of $v_\theta(\theta, t) = 0$ at time $t = t_\theta$ and α_θ is the corresponding LOS-fixed flight-path angle. Recall from Sec. II.C that

$$\gamma_{n_T}(t)t = \int_0^t K_2(\tau)a_{n_T}(\tau)\,\mathrm{d}\tau$$

Note that $K_2 = 0$ gives the PPN law, whereas $K_2 \neq 0$ gives the APPN law. Therefore, from inequality (12) and Eq. (21),

$$\begin{aligned}&[-\phi_0 - n\pi - \gamma_{n_T}(t_\theta)t_\theta - \sin^{-1}(1/\nu)]/k \le (\alpha_\theta - \gamma_{n_T}(t_\theta)t_\theta - \phi_0)/k \\ &\quad \le [-\phi_0 - n\pi - \gamma_{n_T}(t_\theta)t_\theta + \sin^{-1}(1/\nu)]/k \\ &\quad \Rightarrow -n\pi - \sin^{-1}(1/\nu) \le \alpha_\theta \le -n\pi + \sin^{-1}(1/\nu) \end{aligned} \quad (22)$$

where $n = 0, \pm1, \pm2, \ldots$. From the inequality (22), at any time t, corresponding to $S_\theta^-(t)$ and $S_\theta^+(t)$ sectors, respectively, in the target-centered coordinate system, two sectors $S_\alpha^-(t)$ and $S_\alpha^+(t)$ can be obtained as follows:

$$\begin{aligned}S_\alpha^-(t) &= \{\alpha_\theta : -\sin^{-1}(1/\nu) \le \alpha_\theta \le \sin^{-1}(1/\nu)\}; \\ S_\alpha^+(t) &= \{\alpha_\theta : -\pi - \sin^{-1}(1/\nu) \le \alpha_\theta \le -\pi + \sin^{-1}(1/\nu)\}\end{aligned} \quad (23)$$

Clearly, for both PPN and APPN, these sectors $S_\alpha^-(t)$ and $S_\alpha^+(t)$ depend only on the speed ratio ν. They are independent of the initial conditions, target maneuver, and time. Therefore, in the subsequent analysis, these sectors will be referred to as S_α^- and S_α^+, respectively. The sectors S_α^- and S_α^+ are represented in Fig. 5. Also note that, by ([16] Theorem 1) and ([18] Theorem 1), in the case of PPN and by Lemma 4 in this paper in the case of APPN, if the interceptor velocity vector is within the S_α^- sector at any time t, the normalized range rate $v_R(t) < 0$ and the interceptor velocity vector remains within the S_α^- sector for all subsequent time until interception. From ([16] Theorems 1 and 2) and ([18] Corollaries 1 and 2), it is evident that, if the interceptor velocity vector is within the S_α^+ sector at any time t, then the capture of the maneuvering target by PPN guidance law is not guaranteed, in general, except with some additional conditions on the navigation gain N and initial LOS rate $\dot{\theta}_0$. Thus, S_α^- and S_α^+ represent the neighborhoods of the collision course and inverse collision course in the interceptor-centered LOS reference frame. The normalized relative velocity equations at the initial time $t = 0$ can be obtained from Eqs. (9) and (10) as

$$v_{R_0} = \cos(-\theta_0) - \nu\cos(\alpha_0) = \cos(\theta_0) - \nu\cos(\alpha_0) \quad (24)$$

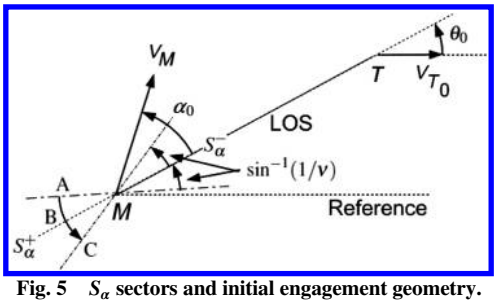

Fig. 5 S_α sectors and initial engagement geometry.

$$v_{\theta_0} = \sin(-\theta_0) - \nu\sin(\alpha_0) = -\sin(\theta_0) - \nu\sin(\alpha_0) \quad (25)$$

From Eqs. (24) and (25), the equation of a circle, which defines all possible combinations of v_{R_0} and v_{θ_0} for a given initial LOS angle θ_0 and speed ratio ν, is obtained as in Eq. (26), and a set S_1 of all such points for $\theta_0 \in [-\pi, \pi)$ is defined as in Eq. (27):

$$(v_{R_0} - \cos\theta_0)^2 + (v_{\theta_0} + \sin\theta_0)^2 = \nu^2 \quad (26)$$

$$\begin{aligned}S_1 \triangleq \{&(v_{\theta_0}, v_{R_0}) | (v_{R_0} - \cos(\theta_0))^2 + (v_{\theta_0} + \sin(\theta_0))^2 \\ &= \nu^2 \text{for} \theta_0 \in [-\pi, \pi)\}\end{aligned} \quad (27)$$

Also, note that the relative speed of the interceptor with respect to the target is bounded above by $V_M + V_T$ and below by $V_M - V_T$, that is,

$$\nu - 1 \le \sqrt{v_R^2 + v_\theta^2} \le \nu + 1$$

Therefore, for a given speed ratio ν, all possible combinations of v_{R_0} and v_{θ_0} lie in a disk, the internal and external radius of which are given as $\nu - 1$ and $\nu + 1$, respectively. Now, define a set S_2 as

$$S_2 \triangleq \{(v_{\theta_0}, v_{R_0}) | (\nu - 1)^2 \le v_{\theta_0}^2 + v_{R_0}^2 \le (\nu + 1)^2\} \quad (28)$$

For any $\theta_0 \in [-\pi, \pi)$, any element $(v_{\theta_0}, v_{R_0}) \in S_1$ can be expressed as $(\cos(\theta_0) + \nu\sin\psi, -\sin(\theta_0) + \nu\cos\psi)$, where $\psi \in [-\pi, \pi)$. Then, for any element in S_1,

$$\begin{aligned}v_{\theta_0}^2 + v_{R_0}^2 &= 1 + \nu^2 + 2\nu\sin(\psi - \theta_0) \\ &\Rightarrow (\nu - 1)^2 \le v_{\theta_0}^2 + v_{R_0}^2 \le (\nu + 1)^2\end{aligned} \quad (29)$$

Therefore, $S_1 \subseteq S_2$. On the other hand, any element $(v_{\theta_0}, v_{R_0}) \in S_2$ can be represented as $(C\cos\psi, C\sin\psi)$, where $\nu - 1 \le C \le \nu + 1$ and $\psi \in [-\pi, \pi)$. Since $-1 \le [(\nu^2 - 1) - C^2]/2C \le 1$, for any element in S_2, there exists a $\theta_0 \in [-\pi, \pi)$ such that the following equation holds good:

$$(v_{R_0} - \cos(\theta_0))^2 + (v_{\theta_0} + \sin(\theta_0))^2 = C^2 + 2C\sin(\theta_0 - \psi) + 1 = \nu^2 \quad (30)$$

Therefore, $S_2 \subseteq S_1$. This implies that

$$S_1 = S_2 \quad (31)$$

B. Guaranteed Capture Zone of PPN in the Normalized Relative Velocity Space

Let the guaranteed capture zone of PPN against a target executing a piecewise continuous maneuver be denoted as CR_{PPN}. As noted in Sec. IV.A, if the interceptor velocity vector is within S_α^+ sector at any time t, then the capture of the maneuvering target is not guaranteed by PPN in general. From Eq. (23), for a given θ_0 and ν, the S_α^+ sector can be represented as an arc on the circle given by Eq. (26). Points on this arc do not fall in CR_{PPN}. From Figs. 5 and 6, note that, for a given θ_0 and ν, at the extreme points "A" and "C" and the center point "B" of the arc, $\alpha_0|_A = -\pi - \sin^{-1}(1/\nu)$, $\alpha_0|_C = -\pi + \sin^{-1}(1/\nu)$ and $\alpha_0|_B = -\pi$, respectively. Therefore,

$$\begin{aligned}&v_{\theta_0}|_A = -(1 + \sin\theta_0); \quad v_{R_0}|_A = \cos\theta_0 + \nu\cos(\sin^{-1}(1/\nu)) \\ &v_{\theta_0}|_B = -\sin\theta_0; \quad v_{R_0}|_B = \cos\theta_0 + \nu \\ &v_{\theta_0}|_C = (1 - \sin\theta_0); \quad v_{R_0}|_C = \cos\theta_0 + \nu\cos(\sin^{-1}(1/\nu))\end{aligned} \quad (32)$$

From Eqs. (26) and (32), for a given ν and θ_0, the possible combinations of v_{R_0} and v_{θ_0} are depicted in Fig. 6, indicating the points inside and outside the S_α^+ sector. From Eq. (32), it is evident

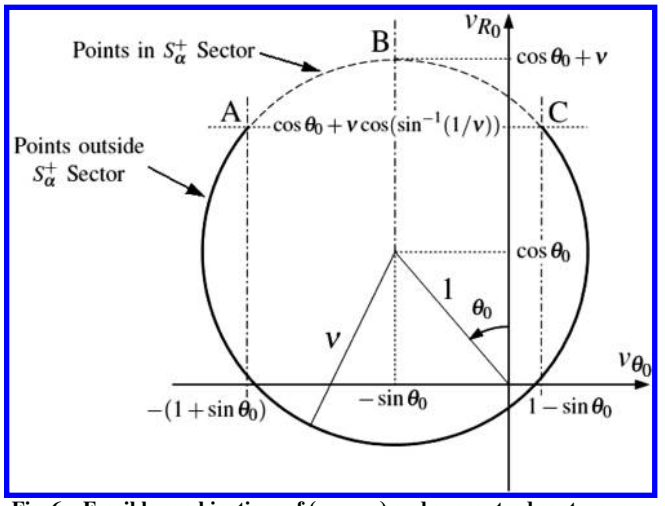

Fig. 6 Feasible combinations of (v_{θ_0}, v_{R_0}) and guaranteed capture zone of PPN for a given ν and θ_0.

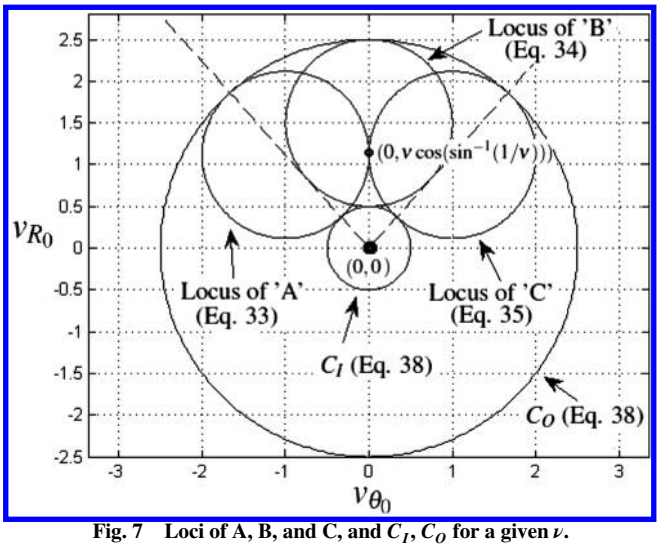

Fig. 7 Loci of A, B, and C, and C_I, C_O for a given ν.

that, for a given ν and different values of $\theta_0 \in [-\pi, \pi)$, the points A, B, and C exist and their loci are the circles with unit radius, respectively, as obtained here:

$$[v_{R_0}|_A - \nu\cos(\sin^{-1}(1/\nu))]^2 + (v_{\theta_0}|_A + 1)^2 = 1 \tag{33}$$

$$(v_{R_0}|_B - \nu)^2 + v_{\theta_0}|_B^2 = 1 \tag{34}$$

$$[v_{R_0}|_C - \nu\cos(\sin^{-1}(1/\nu))]^2 + (v_{\theta_0}|_C - 1)^2 = 1 \tag{35}$$

For a given ν and $\theta_0 \in [-\pi, \pi)$, the curve representing the points in the guaranteed capture zone in the relative velocity space originates from the corresponding point on the circle in Eq. (33) and ends at the corresponding point on the circle in Eq. (35). The points on the arc "ABC" have $v_{R_0} \geq v_{R_0}|_A = v_{R_0}|_C = \cos\theta_0 + \nu\cos(\sin^{-1}(1/\nu))$. Therefore, from Eqs. (32–35), for a given ν and any $\theta_0 \in [-\pi, \pi)$, in the guaranteed capture zone $v_{R_0} \leq v_{R_0}|_A = v_{R_0}|_C = \cos\theta_0 + \nu\cos(\sin^{-1}(1/\nu))$. Hence, the guaranteed capture zone of PPN against maneuvering target CR_{PPN} can be written as

$$CR_{\text{PPN}} = \{(v_{\theta_0}, v_{R_0}) | (v_{R_0} - \cos(\theta_0))^2 + (v_{\theta_0} + \sin(\theta_0))^2 = \nu^2, v_{R_0} < \cos(\theta_0) + \nu\cos(\sin^{-1}(1/\nu)) \text{ for } \theta_0 \in [-\pi, \pi)\} \tag{36}$$

In other words, for a given θ_0 and ν, the points $(-\sin\theta_0 - \nu\sin\phi, \cos\theta_0 + \nu\cos\phi)$ lie in the guaranteed capture zone for all $\phi \in [-\pi, \pi)$, except for $\phi \in (-\sin^{-1}(1/\nu), \sin^{-1}(1/\nu))$, which corresponds to the S_α^+ sector. Hence, Eq. (36) can be equivalently written as

$$CR_{\text{PPN}} = \{(v_{\theta_0}, v_{R_0}) | v_{\theta_0} = -\sin\theta_0 - \nu\sin\phi, v_{R_0} = \cos\theta_0 + \nu\cos\phi \text{ for } \phi \in \{[-\pi, -\sin^{-1}(1/\nu)] \cup [\sin^{-1}(1/\nu), \pi)\}, \theta_0 \in [-\pi, \pi)\} \tag{37}$$

Also, define two circles in the (v_{θ_0}, v_{R_0}) plane with center at origin and radii $\nu - 1$ and $\nu + 1$ as C_I and C_O, respectively:

$$C_I \triangleq \{(v_{\theta_0}, v_{R_0}) | v_{R_0}^2 + v_{\theta_0}^2 = (\nu - 1)^2\};$$
$$C_O \triangleq \{(v_{\theta_0}, v_{R_0}) | v_{R_0}^2 + v_{\theta_0}^2 = (\nu + 1)^2\} \tag{38}$$

Circles representing the loci of A, B, and C in Eqs. (33–35) and C_I, C_O in Eq. (38) are shown in Fig. 7 for a given ν. Now, the boundary of the guaranteed capture zone of PPN against a maneuvering target would be determined. For a given θ_0 and ν, the value of $v_{\theta_0}^2 + v_{R_0}^2$ at a point on the guaranteed capture zone is given as $\nu^2 + 1 + 2\nu\cos(\phi - \theta_0)$, which is higher when ϕ is closer to θ_0. From Eq. (37), for the circles in Eq. (26) for $\theta_0 \in (-\sin^{-1}(1/\nu), 0)$, in CR_{PPN}, $v_{\theta_0}^2 + v_{R_0}^2$ is maximum for $\phi = -\sin^{-1}(1/\nu)$, which corresponds to the points on the circle in Eq. (35). Similarly, for the circles in Eq. (26) for $\theta_0 \in [0, \sin^{-1}(1/\nu))$, in CR_{PPN}, $v_{\theta_0}^2 + v_{R_0}^2$ is maximum for $\phi = \sin^{-1}(1/\nu)$, which corresponds to the points on the circle in Eq. (33). However, for the circles in Eq. (26) for $\theta_0 \in \{[-\pi, -\sin^{-1}(1/\nu)] \cup [\sin^{-1}(1/\nu), \pi)\}$, in CR_{PPN}, the maximum value of $v_{\theta_0}^2 + v_{R_0}^2$ is equal to $(\nu + 1)^2$, which is obtained at $\phi = \theta_0$.

Also, $v_{\theta_0}^2 + v_{R_0}^2$ is minimum and equal to $(\nu - 1)^2$ for $|\phi - \theta_0| = \pi$. Therefore, for $\theta_0 \in [-\pi + \sin^{-1}(1/\nu), \pi - \sin^{-1}(1/\nu)]$, any circle in Eq. (26) touches C_I at a point. But for $\theta_0 \in \{(-\pi, -\pi + \sin^{-1}(1/\nu)), (\pi - \sin^{-1}(1/\nu), \pi)\}$, the circles in Eq. (26) do not touch C_I at any point, because the angle ϕ, which satisfies $|\phi - \theta_0| = \pi$ in these circles, lie in the interval $(-\sin^{-1}(1/\nu), \sin^{-1}(1/\nu))$, which does not fall in CR_{PPN}, as can be noted from Eq. (37).

Thus, for a given $\nu > \sqrt{2}$ and $k\nu > 1$, we find the following five mutually exclusive and exhaustive cases of θ_0. As mentioned earlier, for any $\theta_0 \in [-\pi, \pi)$, the candidate points on the circle in Eq. (26) for guaranteed capture zone CR_{PPN} have their two ends A and C on the two circles, given by Eqs. (33) and (35), respectively.

1) For any θ_0 in the interval $0 \leq \theta_0 \leq \sin^{-1}(1/\nu)$, A and C on the circle in Eq. (26) form the outer envelope boundary points, and the circle also touches C_I at a point at an angle $-\pi + \theta_0$ with respect to the v_{R_0} axis, which forms the inner envelope boundary point.

2) For any θ_0 in the interval $\sin^{-1}(1/\nu) < \theta_0 \leq \pi - \sin^{-1}(1/\nu)$, C on the circle in Eq. (26) forms one of the outer envelope boundary points. The circle touches C_O and C_I at two points at angle θ_0 and $-\pi + \theta_0$, respectively, with respect to the v_{R_0} axis. They form one outer envelope and one inner envelope boundary point, respectively.

3) For any θ_0 in the interval $\theta_0 \in \{(-\pi, -\pi + \sin^{-1}(1/\nu)) \cup (\pi - \sin^{-1}(1/\nu), \pi)\}$, neither A nor C on the circle in Eq. (26) forms the outer envelope boundary points. The circle touches C_O at a point at angle θ_0, with respect to the v_{R_0} axis, which forms one outer envelope boundary point.

4) For any θ_0 in the interval $-\pi + \sin^{-1}(1/\nu) \leq \theta_0 \leq -\sin^{-1}(1/\nu)$, A on the circle in Eq. (26) forms one of the outer envelope boundary points. The circle touches C_O and C_I at two points at angles θ_0 and $-\pi + \theta_0$ (modulo 2π), respectively, with respect to the v_{R_0} axis. They form one outer envelope point and one inner envelope boundary point, respectively.

5) For any θ_0 in the interval $-\sin^{-1}(1/\nu) \leq \theta_0 < 0$, A and C on the circle in Eq. (26) form the outer envelope boundary points. The circle touches C_I only at a point at angle $-\pi + \theta_0$ with respect to the v_{R_0} axis, which forms the inner envelope boundary point.

Any point in the normalized relative velocity space, that is, the (v_{θ_0}, v_{R_0}) plane, can be represented as $(-K\sin\psi, K\cos\psi)$, where

$$K = \sqrt{v_{\theta_0}^2 + v_{R_0}^2} \in [\nu - 1, \nu + 1]$$

and the angle ψ is considered with respect to the v_{R_0} axis. In the (v_{θ_0}, v_{R_0}) plane, define three sets S_3, S_4, and S_5 as

$$S_3 \triangleq \{(v_{\theta_0}, v_{R_0}) | v_{\theta_0}^2 + v_{R_0}^2 \geq (\nu - 1)^2; (v_{R_0} - \nu \cos(\sin^{-1}(1/\nu)))^2 + (v_{\theta_0} - 1)^2 \leq 1 \quad \text{for } \psi \in (-\sin^{-1}(1/\nu), 0)\} \tag{39}$$

$$S_4 \triangleq \{(v_{\theta_0}, v_{R_0}) | v_{\theta_0}^2 + v_{R_0}^2 \geq (\nu - 1)^2; (v_{R_0} - \nu \cos(\sin^{-1}(1/\nu)))^2 + (v_{\theta_0} + 1)^2 \leq 1 \quad \text{for } \psi \in [0, \sin^{-1}(1/\nu))\} \tag{40}$$

$$S_5 \triangleq \{(v_{\theta_0}, v_{R_0}) | (\nu - 1)^2 \leq v_{\theta_0}^2 + v_{R_0}^2 \leq (\nu + 1)^2 \quad \text{for } \psi \in [-\pi, -\sin^{-1}(1/\nu)] \cup [\sin^{-1}(1/\nu), \pi)\} \tag{41}$$

From the five mutually exclusive and exhaustive cases of θ_0, it is evident that, along any angle $\psi \in \{[-\pi, -\sin^{-1}(1/\nu)] \cup [\sin^{-1}(1/\nu), \pi]\}$, with respect to the v_{R_0} axis, the outer and inner envelope boundaries are formed by points on C_O and C_I, respectively, which implies that S_5, defined in Eq. (41), forms a part of the guaranteed capture zone CR_{PPN}. Also, along any angle ψ belonging to the intervals $(-\sin^{-1}(1/\nu), 0)$ and $(0, \sin^{-1}(1/\nu))$, with respect to the v_{R_0} axis, the boundaries are formed by the points on the circles given by Eqs. (35) and (33), respectively. Along the angle $\psi = 0$, with respect to the v_{R_0} axis, the outer and inner envelope boundaries merge at a point $(0, \nu \cos(\sin^{-1}(1/\nu)))$, at which the circles given by Eqs. (35) and (33) touch each other. This implies that S_3 and S_4, defined in Eqs. (39) and (40), respectively, form the rest of the guaranteed capture zone CR_{PPN}. The analysis given earlier leads to the following theorem.

Theorem 4: Consider an ideal interceptor, guided by standard PPN guidance law with navigation gain N and interceptor speed V_M, pursuing a maneuvering target with speed V_T and piecewise continuous maneuver $a_T(t)$ such that $\nu > \sqrt{2}$ and $k\nu > 1$. For a given ν, the guaranteed capture zone of the PPN-guided interceptor in the normalized relative velocity space is given as

$$CR_{\text{PPN}} = S_3 \cup S_4 \cup S_5 \tag{42}$$

where S_3, S_4, and S_5 are given by Eqs. (39–41), respectively.

Proof: From the discussion presented earlier, this result is straightforward. □

From Theorem 4, the guaranteed capture zone CR_{PPN} and its boundary in the (v_{θ_0}, v_{R_0}) plane are depicted for a given ν (= 1.5) in Fig. 8, where the sets S_3, S_4, and S_5 are also marked. Guaranteed capture zones for $\theta_0 = 0, \pi/2$, and $-\pi$ (corresponding to cases 1, 2, and 3 of θ_0 mentioned earlier) are indicated in Fig. 8. Clearly, by Eqs. (27), (28), (31), (37), and (39–42), $CR_{\text{PPN}} \subset S_1 = S_2$.

C. Guaranteed Capture Zone of APPN in Normalized Relative Velocity Space

Theorem 5: Consider an ideal interceptor, guided by APPN guidance law with navigation gain N, interceptor speed V_M, and augmentation parameter $K_1(t)$, pursuing a maneuvering target with speed V_T and piecewise continuous maneuver $a_T(t)$ such that $\nu > \sqrt{2}$, $N > 2 + 2/\sqrt{\nu^2 - 1} > 1 + 1/\nu$, $\text{sgn}(K_1(t)) = \text{sgn}(a_T\dot{\theta}(t))$, and $|K_1(t)| > 1/\sqrt{1 - 1/\nu^2}$. Then, for a given ν, the guaranteed capture zone of the APPN-guided interceptor in the normalized relative velocity space is given as

$$CR_{\text{APPN}} = \{(v_{\theta_0}, v_{R_0}) | (\nu - 1)^2 \leq v_{\theta_0}^2 + v_{R_0}^2 \leq (\nu + 1)^2\} \tag{43}$$

Proof: From Theorems 1 and 2, it is evident that, if all the conditions stated in this theorem are satisfied, then successful interception of the target, executing a bounded and piecewise continuous maneuver, can be achieved from any initial engagement geometry. Therefore, from Eqs. (26–28), for a given speed ratio ν, the guaranteed capture zone of APPN against a maneuvering target is given as $CR_{\text{APPN}} = S_2 = \{(v_{\theta_0}, v_{R_0}) | (\nu - 1)^2 \leq v_{\theta_0}^2 + v_{R_0}^2 \leq (\nu + 1)^2\}$. □

From Theorem 5, for $\nu = 1.5$, CR_{APPN} and its boundary in the (v_{θ_0}, v_{R_0}) plane are shown in Fig. 9, along with the guaranteed capture zone for $\theta_0 = 0$, which is a circle given by Eq. (26) with $\theta_0 = 0$. From Eqs. (27), (28), and (39–43), clearly, the guaranteed capture zone of PPN is a subset of that of APPN in normalized initial relative velocity space, that is, $CR_{\text{PPN}} = S_3 \cup S_4 \cup S_5 \subset CR_{\text{APPN}} = S_2$.

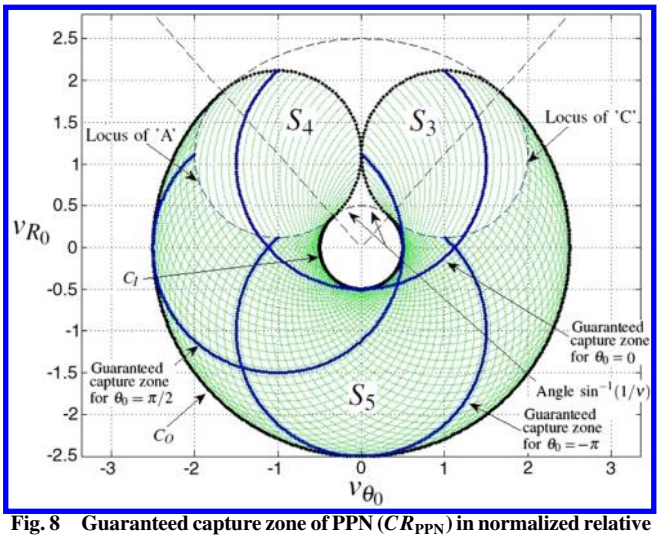

Fig. 8 Guaranteed capture zone of PPN (CR_{PPN}) in normalized relative velocity plane for a given ν.

V. Simulation Results

Simulation results are shown for the following engagement parameters: $V_M = 1500$ and $V_T = 1000$ m/s (and hence, $\nu = 1.5$), initial range $\rho_0 = 10,000$ m, and $\alpha_{T_0} = 0$. In the variable target maneuver case, shown in Figs. 10 and 11, the target performs a sinusoidal maneuver with $a_T = 3g \sin(\pi t/10)$, whereas in the constant target maneuver case, shown in Fig. 12, the target performs a constant maneuver with $a_T = 3g$. In Figs. 10–12, simulation results are shown for three guidance laws: APPN (presented in this paper), standard PPN, and augmented PN motivated by the optimum guidance law of Garber [20] [referred to as "OGL (Garber [20])" in the subsequent discussion].

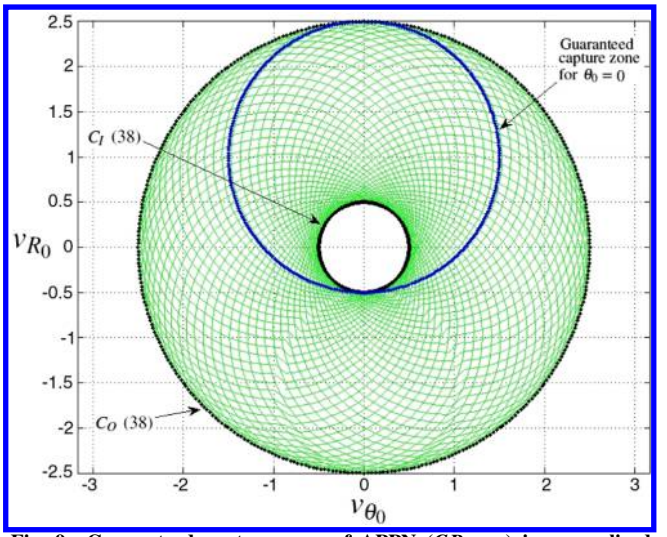

Fig. 9 Guaranteed capture zone of APPN (CR_{APPN}) in normalized relative velocity plane for a given ν.

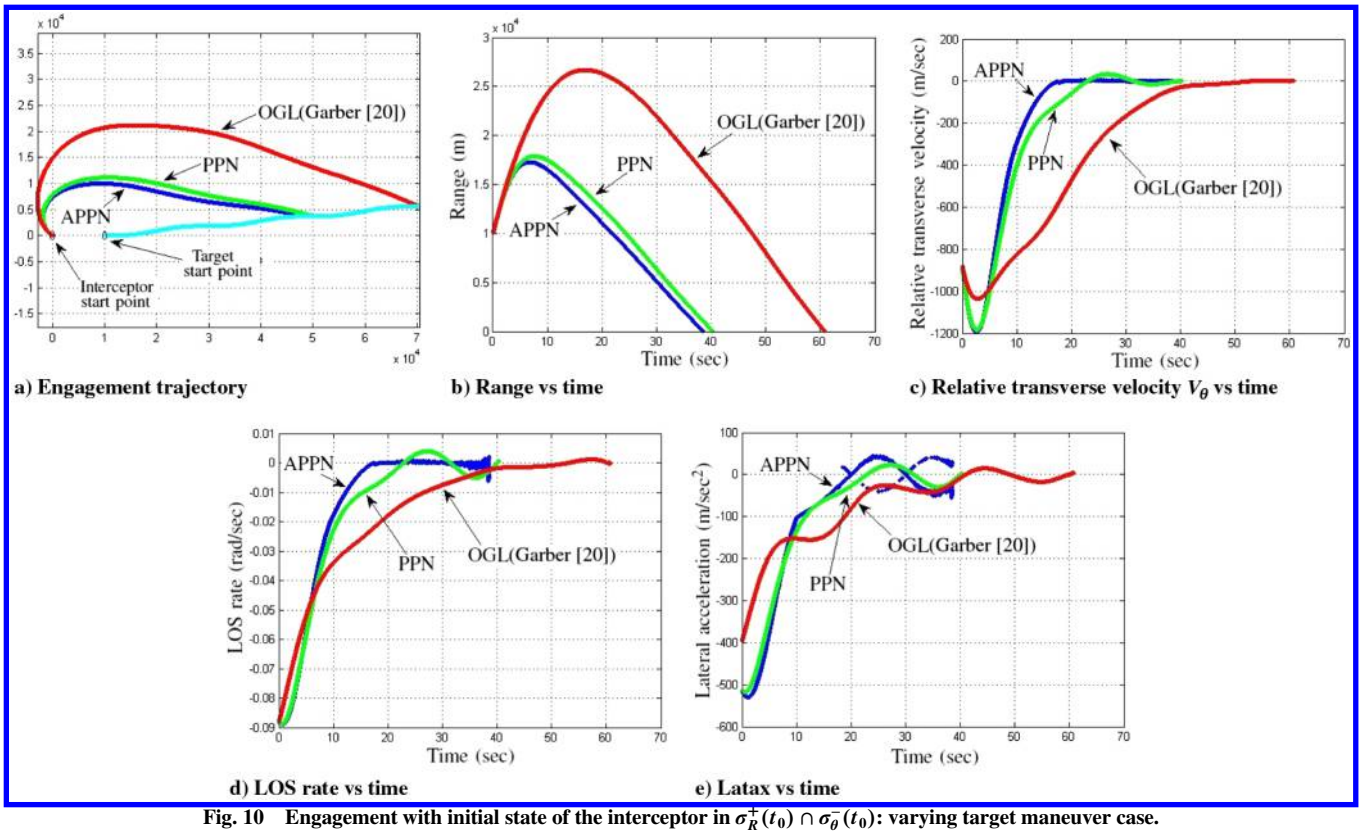

Fig. 10 Engagement with initial state of the interceptor in $\sigma_R^+(t_0) \cap \sigma_\theta^-(t_0)$: varying target maneuver case.

A. Piecewise Continuous Bounded Target Maneuver

In this section, the navigation gain used for APPN and standard PPN is $N = 2 + (2V_T/\sqrt{V_M^2 - V_T^2}) + 0.1 = 3.889$, and for OGL (Garber) [20] is 3. Augmentation parameter $K_1 = K_2\nu = 1.357\text{sgn}(a_T\dot{\theta})$, where $K_2 = \text{sgn}(a_T\dot{\theta})(1/\sqrt{\nu^2 - 1 + 0.01}) = 0.905\text{sgn}(a_T\dot{\theta})$. The engagement trajectories of the interceptor and target, variation of range ρ, relative transverse velocity V_θ, LOS turn rate $\dot{\theta}$, and lateral acceleration command a_M with time are shown for $M_0(r_0, \theta_0) \in \sigma_R^+(t_0) \cap \sigma_\theta^-(t_0)$ $(\theta_0 = 0, \alpha_{M_0} = 0.8\pi)$ and $M_0(r_0, \theta_0) \in S_\theta^+(t_0)$ $(\theta_0 = 0, \alpha_{M_0} = \pi)$ in Figs. 10 and 11, respectively, for variable target maneuver, and for $M_0(r_0, \theta_0) \in \sigma_R^+(t_0) \cap \sigma_\theta^-(t_0)$ $(\theta_0 = 0, \alpha_{M_0} = 0.8\pi)$ in Fig. 12 for constant target

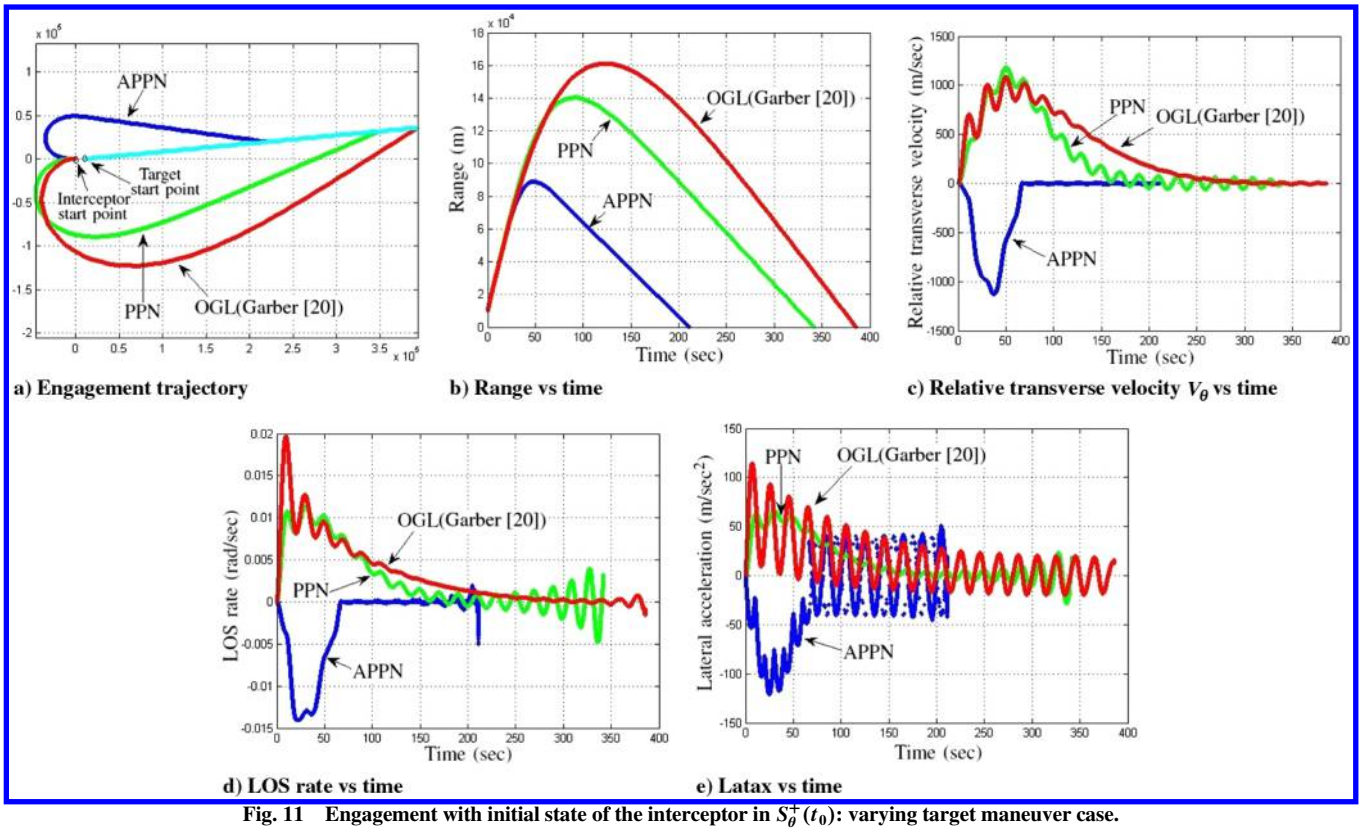

Fig. 11 Engagement with initial state of the interceptor in $S_\theta^+(t_0)$: varying target maneuver case.

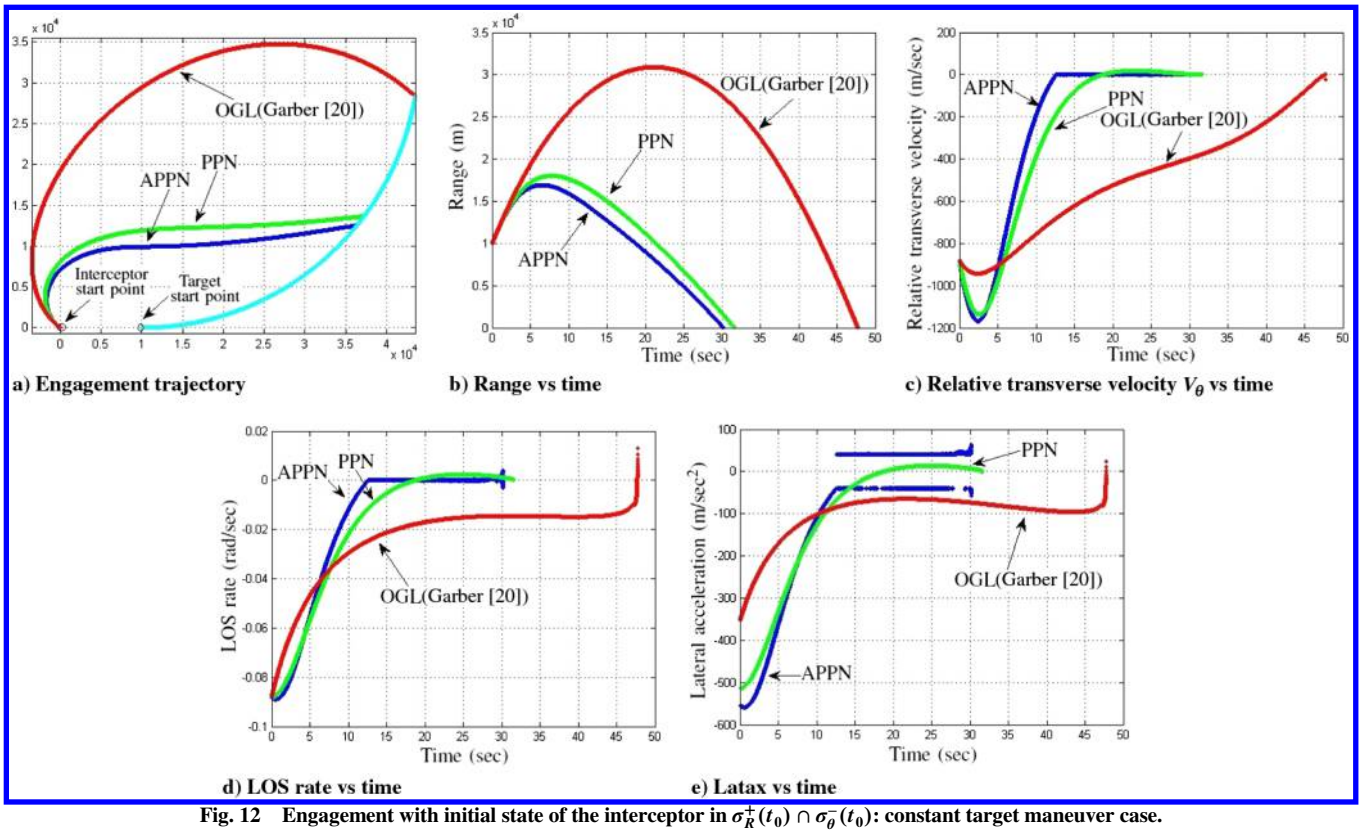

Fig. 12 Engagement with initial state of the interceptor in $\sigma_R^+(t_0) \cap \sigma_\theta^-(t_0)$: constant target maneuver case.

maneuver. Simulation results in Figs. 10–12 validate the results of successful interception of the target maneuvering with a bounded and piecewise continuous lateral acceleration by the APPN-guided interceptor in Theorems 1 and 2 and Corollary 1, respectively.

From Figs. 10b, 11b, and 12b, it is clear that the interceptor, when guided by the APPN guidance law, reaches the target faster than for PPN-guided ones, as indicated in the subsequent discussions of Theorems 1 and 2. This difference in the final time t_f is more vividly clear in the case when the engagement begins with M in the $S_\theta^+(t_0)$ region in the polar plane, as can be seen from Fig. 11. Also, it should be noted from Figs. 10b, 11b, and 12b that this difference in t_f is significant when APPN guidance law is compared with OGL (Garber) [20]. This is mainly because the augmentation parameter, that is, the coefficient associated with the target maneuver in the

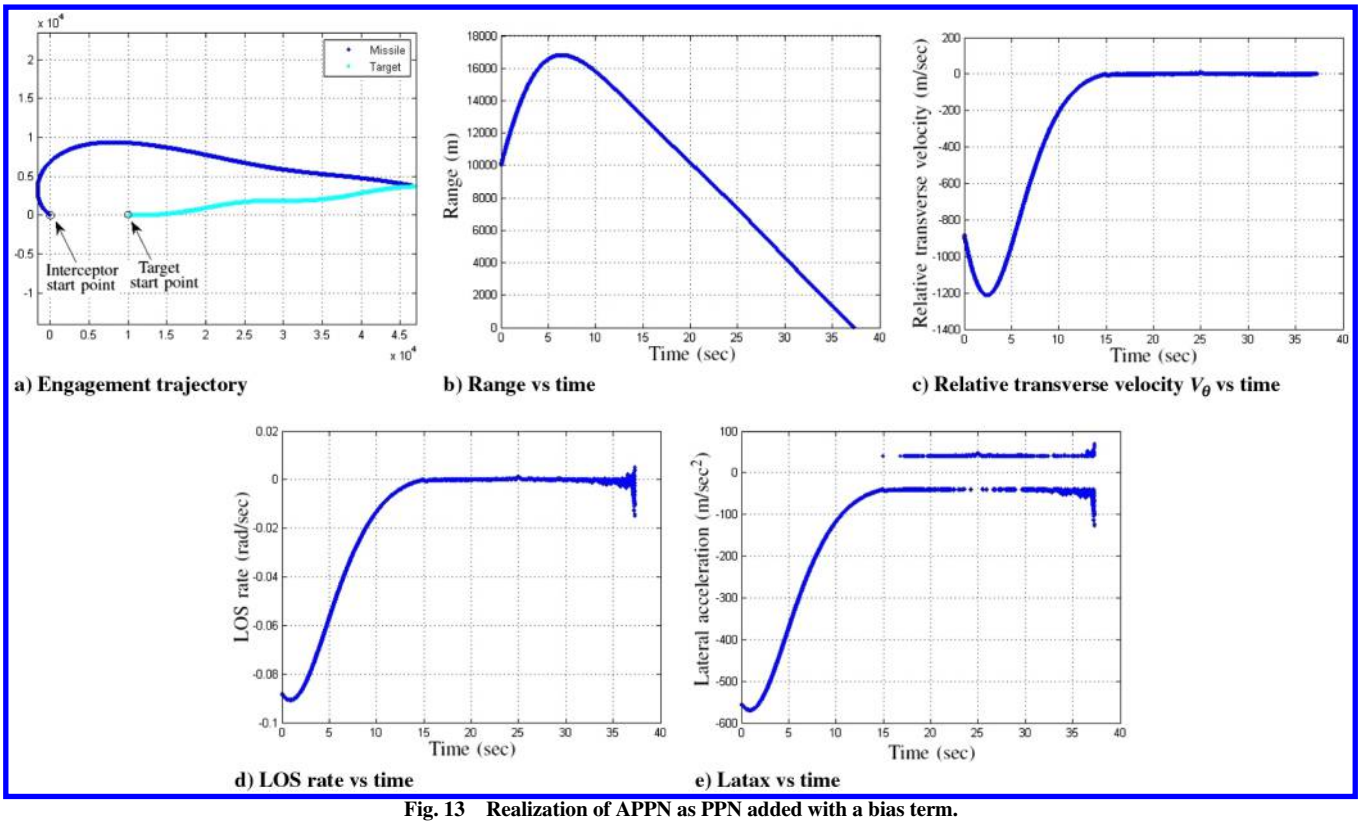

Fig. 13 Realization of APPN as PPN added with a bias term.

guidance command is fixed in the case of OGL (Garber [20]), whereas this parameter varies in the case of APPN in a way such that the angular rotation of the sectors in the polar plane is used in favor of faster approach of M toward the $v_\theta(\theta, t) = 0$ isocurve in the $S_\theta^-(t)$ sector for some $t > t_0$, as can be noted from Figs. 10c, 11c, and 12c. During the endgame of the engagement, when M is very close to the $v_\theta(\theta, t) = 0$ isocurve in the $S_\theta^-(t)$ sector, then in the neighborhood of the zero LOS rate line, $\dot{\theta}$ undergoes chattering about zero, as observed in Figs. 10d, 11d, and 12d. For the variable target maneuver case, this leads to chattering with frequent jumps and changes in sign in the lateral acceleration profile of the APPN-guided interceptor during the later part of the engagement, as can be seen from Figs. 10e and 11e. On the other hand, for the constant target maneuver case, the chattering of $\dot{\theta}$ about zero in the endgame leads to a chattering in $a_M(t)$ about the twin surface $a_M = \pm\hat{a}_M = \pm 39.937$, as observed from Fig. 12e. These justify the discussion subsequent to Theorem 3 and Corollary 1, respectively.

B. Simplified Realization of APPN as PPN with a Bias Term

The navigation gain used for the simplified APPN Eq. (A16) is $N = 2 + (2V_T/\sqrt{V_M^2 - V_T^2}) + 0.1 = 3.889$. The sinusoidal target maneuver $a_T = 3g\ \sin(\pi t/10)$ is considered. Therefore, the bias term in a_M is $C_2 = 3g|K_1| = 39.937$, where $K_1 = K_2\nu = \text{sgn}(a_T\dot{\theta})\nu(1/\sqrt{\nu^2 - 1} + 0.01) = 1.357\text{sgn}(a_T\dot{\theta})$. The simulation result for the simplified realization of APPN is shown in Fig. 13 for $M_0(r_0, \theta_0) \in \sigma_R^+(t_0) \cap \sigma_\theta^-(t_0)$ $(\theta_0 = 0, \alpha_{M_0} = 0.8\pi)$ which validates the results in Corollary 2 on the realization of APPN guidance law as PPN added with a bias term, magnitude and sign of which depend on $a_{T_{\max}}$ and sign of $\dot{\theta}$, respectively. The bias term based on the a priori information about the maximum capability of the target's maneuver in this simplified formulation of APPN increases the relative angular rate of M with respect to the sectors in the polar plane compared with the case of APPN in Eq. (6), leading to a faster approach toward zero LOS rate and even faster interception, which can be observed from Figs. 10b, 10d, 13b, and 13d. Also, note that, because this realization of APPN as PPN added with a bias term resembles APPN in Eq. (6), where $a_T(t)$ is equal to $a_{T_{\max}}$ for all time t during the engagement, the lateral acceleration profile in Fig. 13e is similar to the constant maneuver target case in Fig. 12e.

C. Implementation of APPN + PPN

The simulation result on the implementation of APPN+PPN guidance against a target executing a sinusoidal maneuver $a_T = 3g\ \sin(\pi t/10)$ is shown in Fig. 14, which validates the discussion in Sec. III.F. The initial engagement geometry $M_0(r_0, \theta_0) \in \sigma_R^+(t_0) \cap \sigma_\theta^-(t_0)$ $(\theta_0 = 0, \alpha_{M_0} = 0.8\pi)$. Use of APPN until M reaches the $S_\theta^-(t)$ sector at some finite $t > t_0$ has been instrumental in faster approach of M toward the $S_\theta^-(t)$ sector in the polar plane. When the LOS rate reaches close to zero, the augmentation parameter K_1 is made zero, which implies that only the PPN term is active then onward until interception, leading to a smooth and bounded lateral acceleration profile at the terminal phase of the engagement. Another interesting observation from Figs. 10 and 14 is that, with this APPN + PPN in action, the interceptor intercepts the target in slightly less time than in the case of APPN. This is because, when M is very close to the $v_\theta(\theta, t) = 0$ isocurve in the $S_\theta^-(t)$ sector, APPN tries to overcorrect the deviation of M from the $v_\theta(\theta, t) = 0$ isocurve, which, in many cases, leads to more chattering of $\dot{\theta}$ about zero. Therefore, in practical implementation, PPN at the endgame is more beneficial than APPN. Thus, the notion of APPN + PPN guidance, discussed in Sec. III.F, is sufficiently justified.

VI. Conclusions

This paper proposed an augmented PPN guidance law that takes into account target maneuvers. The proposed guidance law is more realistic than the augmentation of any other guidance law of the PN class. Analysis results were presented on a nonlinear framework and dealt with several issues like boundedness of lateral acceleration demand and capturability in relative velocity space. The qualitative analysis approach was used to obtain many of the capturability results. Unlike most results available in the literature, which are confined to analyzing a linearized engagement geometry, this paper addressed the problem using its full nonlinearity without any approximations. The results indicate that the techniques used in the

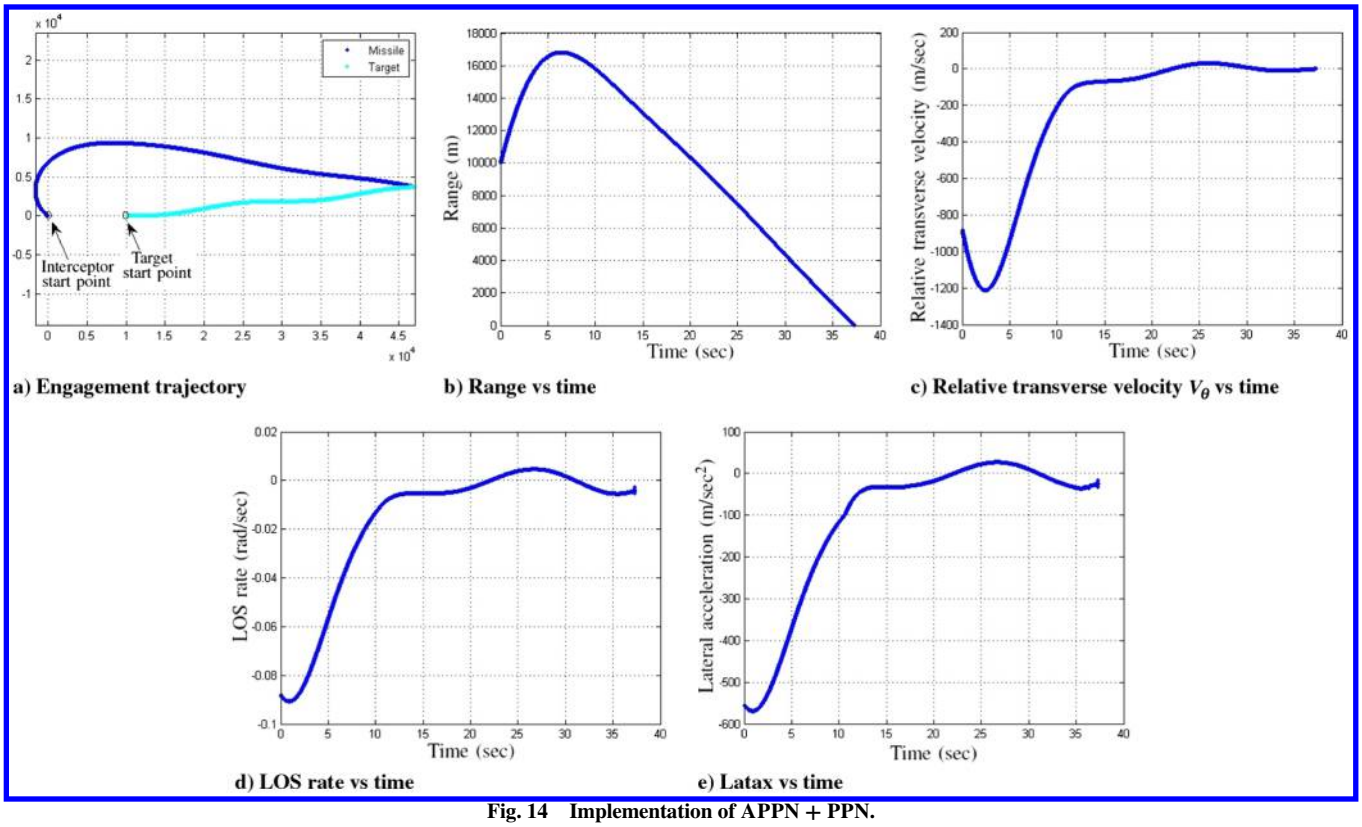

Fig. 14 Implementation of APPN + PPN.

paper can be extended to analyze the performance of other guidance laws in a nonlinear framework. Such results would be close to realistic engagement scenarios and be of more practical use than those obtained in the linearized framework. Future work in this direction can address issues of implementability and the effect of uncertainty.

Appendix: Detailed Proofs

A1 Proof of Lemma 3

First, consider that the interceptor lies in the sector $\sigma_\theta^-(t)$ at some time $t = t_1$ during the engagement. From Fig. 4, at any time t, $\sigma_\theta^-(t)$ can be expressed as the union of three disjoint and exhaustive sets as $\sigma_\theta^-(t) = (\sigma_\theta^-(t) \cap \sigma_R^+(t)) \cup (S_R^-(t)) \cup (\sigma_\theta^-(t) \cap \sigma_R^-(t))$. From ([16] Theorem 1) for a constant target maneuver, and ([18] Theorem 1) for a varying target maneuver, it is evident that, if the sectors do not rotate in the polar plane, then under the conditions $\nu > \sqrt{2}$ and $k\nu > 1$, as θ decreases with time in the $\sigma_\theta^- \cap \sigma_R^+$ region, M first reaches the S_R^- sector and at some finite time $t > t_1$, v_R becomes zero, and then onward v_R becomes negative and, as a result, the trajectory tends to the origin T of the polar plane in the σ_R^- region within some finite time, and finally M arrives at the origin in the polar plane in the S_θ^- sector. However, when the sectors rotate in the polar plane, then, if the relative angular rate $\dot{\theta}_{\text{rel}}(t)$ of M with respect to the sectors in the polar plane is negative and nonzero in the $\sigma_\theta^-(t)$ sector for all subsequent time t, M would enter the sector $S_\theta^-(t)$ at some finite time t.

Consider that, at some time $t = t_1$ during the engagement, M is at an angle $\theta_1 \in (\sigma_\theta^-(t) \cap \sigma_R^+(t))$. Then, $v_\theta(\theta_1, t_1) < 0$ and $v_R(\theta_1, t_1) > 0$. Also, note that the sectors in the polar plane rotate at an angular rate of $-K_2 a_{n_T}(t)/k$ at time t. Therefore, the relative angular rate of M with respect to the sectors in the polar plane is $\dot{\theta}_{\text{rel}}(t) = \dot{\theta}(t) - (-K_2 a_{n_T}(t)/k)$. Since $k = N - 1 > 0$ and in the $\sigma_\theta^-(t)$ sector, $\dot{\theta}(t) < 0$,

$$\text{sgn}(K_1(t)) = \text{sgn}(K_2(t)) = -\text{sgn}(a_T(t)) \Rightarrow -K_2 a_{n_T}(t)/k > 0$$
$$\Rightarrow \dot{\theta}_{\text{rel}}(t) = \dot{\theta}(t) - (-K_2 a_{n_T}(t)/k) < 0 \tag{A1}$$

where K_1 and K_2 are as defined in Sec. II.C. Hence from Eq. (A1), as θ decreases with time in the $\sigma_\theta^-(t)$ sector, if the condition $\text{sgn}(K_1(t)) = \text{sgn}(K_2(t)) = -\text{sgn}(a_T(t))$ holds for all time $t \geq t_1$, then $\dot{\theta}_{\text{rel}}(t)$ is nonzero and negative for all time t. Then, by the integration of piecewise continuous $\dot{\theta}_{\text{rel}}(t)$ over time [34,35], it is obtained that M gradually reaches $S_R^-(t)$ in the polar plane at some finite time $t = t_2 > t_1$ and then $(\sigma_\theta^-(t) \cap \sigma_R^-(t))$ at some finite time $t = t_3 > t_2$. In $(\sigma_\theta^-(t) \cap \sigma_R^-(t))$, as $v_R(t) < 0$, M gradually tends toward the origin of the polar plane T, and, as $\dot{\theta}(t) < 0$ and hence, $\dot{\theta}_{\text{rel}}(t) < 0$ for all time $t > t_3$ that M is in $\sigma_\theta^-(t)$ sector, M enters the $S_\theta^-(t)$ sector in the polar plane within some finite time at $t = t_4 > t_3$.

Next, consider $\sigma_\theta^+(t)$ in which $\dot{\theta}(t) > 0$. From Fig. 4, at any time t, $\sigma_\theta^+(t)$ can be expressed as the union of three disjoint and exhaustive sets as $\sigma_\theta^+(t) = (\sigma_\theta^+(t) \cap \sigma_R^+(t)) \cup (S_R^+(t)) \cup (\sigma_\theta^+(t) \cap \sigma_R^-(t))$. Consider that, at some time $t = t_1$ during the engagement, M is at an angle $\theta_1 \in (\sigma_\theta^+(t) \cap \sigma_R^+(t))$. In this case, by similar argument, if the relative angular rate $\dot{\theta}_{\text{rel}}(t)$ of M with respect to the sectors is positive and nonzero in the $\sigma_\theta^+(t)$ sector for all subsequent time t, then M enters the sector $S_\theta^-(t)$ at some finite time t. Since $k = N - 1 > 0$ and, in the $\sigma_\theta^+(t)$ sector, $\dot{\theta}(t) > 0$,

$$\text{sgn}(K_1(t)) = \text{sgn}(K_2(t)) = \text{sgn}(a_T(t)) \Rightarrow (-K_2 a_{n_T}(t)/k) < 0$$
$$\Rightarrow \dot{\theta}_{\text{rel}}(t) = \dot{\theta}(t) - (-K_2 a_{n_T}(t)/k) > 0 \tag{A2}$$

Hence, if $\text{sgn}(K_1(t)) = \text{sgn}(K_2(t)) = \text{sgn}(a_T(t))$ holds for all time $t \geq t_1$, then by similar argument, M traverses in the direction of increasing θ in the polar plane and reaches $S_R^+(t)$ at some finite time $t = t_2 > t_1$ and then $(\sigma_\theta^+(t) \cap \sigma_R^-(t))$ at some finite time $t = t_3 > t_2$. In $\sigma_R^-(t)$, as $v_R(t) < 0$, M gradually tends toward the origin of the polar plane T, and, as $v_\theta(t) > 0$ and hence, $\dot{\theta}_{\text{rel}}(t) > 0$ for all time $t > t_3$ that M is in the $\sigma_\theta^+(t)$ sector, within some finite time at $t = t_4 > t_3$, M enters the $S_\theta^-(t)$ sector in the polar plane. □

A2 Proof of Lemma 4

From Fig. 4, $S_\theta^-(t) \subset \sigma_R^-(t)$ at any time t during the engagement, that is, while in the sector $S_\theta^-(t)$, M always approaches the origin T in the polar plane. Now, consider that, at time $t = t_1$, M is at some angle $\theta = \theta_1 \in S_\theta^-(t_1)$. Also, $k = N - 1 > 0$. Therefore, if $v_\theta(\theta_1, t_1) < 0 (> 0)$, that is, $\dot{\theta}(t_1) < 0 (> 0)$,

$$\text{sgn}(K_1(t)) = \text{sgn}(K_2(t)) = \text{sgn}(a_T \dot{\theta}(t)) \Rightarrow -K_2 a_{n_T}(t)/k$$
$$> 0 (< 0) \Rightarrow \dot{\theta}_{\text{rel}}(t) = \dot{\theta}(t) - (-K_2 a_{n_T}(t)/k) < 0 (> 0) \tag{A3}$$

From Eq. (A3), if $v_\theta(\theta_1, t_1) < 0 (> 0)$, that is, $\dot{\theta}(t_1) < 0 (> 0)$, then if the condition $\text{sgn}(K_1(t)) = \text{sgn}(a_T \dot{\theta}(t))$ holds for all time $t \geq t_1$, then the relative angular rate of M with respect to the sectors in the polar plane, that is, $\dot{\theta}(t) - (-K_2 a_{n_T}(t)/k)$ is negative (positive), and, in the polar plane M proceeds in the decreasing (increasing) direction of θ until it reaches $\theta = \theta_2$ at some finite time $t = t_2 > t_1$ such that $v_\theta(\theta_2, t_2) = 0$, which follows from a similar argument as in Lemma 3, and hence remains inside the sector $S_\theta^-(t)$ until $t = t_2$.

As $t = t_2 + \varepsilon$ for arbitrarily small $\varepsilon > 0$, the situation of the trajectory of M alters, that is, if $v_\theta(\theta, t) > 0 (< 0)$ for all $t \in [t_1, t_2)$, then at $t = t_2 + \varepsilon$, $v_\theta(\theta, t) < 0 (> 0)$. Following similar arguments, if the condition $\text{sgn}(K_1(t)) = \text{sgn}(a_T \dot{\theta}(t))$ holds for all time $t > t_2$, M remains inside $S_\theta^-(t)$ for $t > t_2$ and reaches the isocurve $v_\theta(\theta, t) = 0$, shown in Fig. A1, at some finite time. This process continues, that is, in the polar plane M oscillates about the isocurve $v_\theta(\theta, t) = 0$ in the $S_\theta^-(t)$ sector for all time t until the range decreases to zero in some finite time, because for any time t, $S_\theta^-(t) \subset \sigma_R^-(t)$ and $v_R(\theta, t)$ is negative and nonzero in the $\sigma_R^-(t)$ sector.

Therefore, if M reaches the sector $S_\theta^-(t)$ in the polar plane at some time $t = t_1$ during the engagement, then if the augmentation parameter $K_1(t)$ is such that $\text{sgn}(K_1(t)) = \text{sgn}(a_T \dot{\theta}(t))$ for all $t \geq t_1$, then M will remain inside the sector $S_\theta^-(t)$ for all time $t > t_1$ during the pursuit until it reaches the origin T of the polar plane. □

A3 Proof of Lemma 6

Clearly, for all time t for which $\dot{\theta}_1$ is as defined in Lemma 6,

$$\dot{\theta}(t) > \dot{\theta}_1(t) (\dot{\theta}(t) < \dot{\theta}_1(t)) \Rightarrow \dot{\theta}(t)$$
$$= \dot{\theta}_1(t) + \dot{\theta}_S(t) (\dot{\theta}(t) = \dot{\theta}_1(t) - \dot{\theta}_S(t)) \tag{A4}$$

where $\dot{\theta}_S(t) > 0$. Substituting $\dot{\theta}$ from Eq. (A4) into Eq. (18), we obtain for all time t

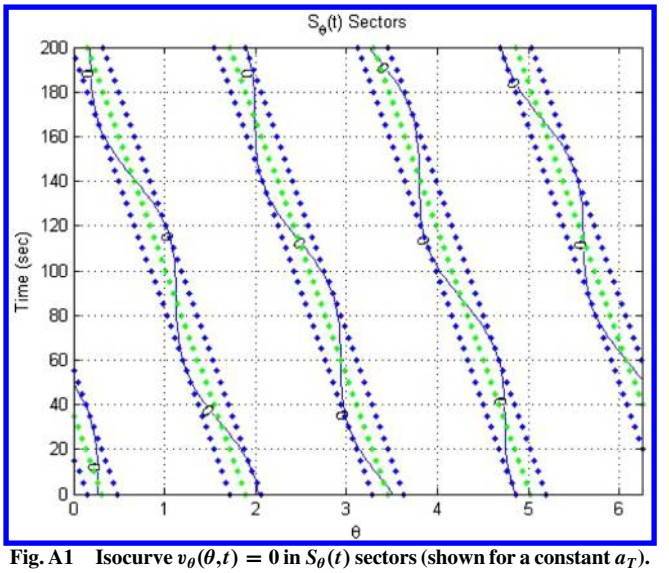

Fig. A1 Isocurve $v_\theta(\theta,t) = 0$ in $S_\theta(t)$ sectors (shown for a constant a_T).

$$R\ddot{\theta} = V_S(t)\dot{\theta}_S \qquad (R\ddot{\theta} = -V_S(t)\dot{\theta}_S) \tag{A5}$$

Because of the continuity of $\dot{\theta}$ in time t, as mentioned in Sec. II.C, from Eq. (A5), clearly, for all time t during the engagement, $\dot{\theta}$ is increasing (decreasing) if $V_S(t) > 0$ and $\dot{\theta}$ is decreasing (increasing) if $V_S(t) < 0$. □

A4 Proof of Theorem 2

From Theorem 1, if Conditions 1–3 of this theorem are satisfied, then the interceptor reaches the target in some finite time from any initial state exterior to $S_\theta^+(t_0)$ in the polar plane. Therefore, it is sufficient to show that, if the conditions mentioned in this theorem are valid, then starting from any $M_0(r_0, \theta_0) \in S_\theta^+(t_0)$, M can go out of the $S_\theta^+(t)$ sector at some finite time $t > t_0$. From Lemma 5 and Condition 2 of this theorem, if M is in $S_\theta^+(t)$ sector in the polar plane at time t, then

$$V_S(t) \geq V_T\left[(N-2)\sqrt{\nu^2-1} - 2\right] = V_e > 0 \tag{A6}$$

Now, define $\dot{\theta}_1$ as

$$\dot{\theta}_1 \triangleq a_T(t)[K_2(t)\nu\cos(k\theta_1 + \gamma_{n_T}(t)t + \phi_0) - \cos(\hat{a}_{n_T}(t)t - \theta_1)]/V_S(t) \tag{A7}$$

Consider first that $a_T(t) > 0, \dot{\theta}(t) > 0$ at some time $t \geq t_0$. Therefore, by Condition 3 of the theorem, $K_2(t) > 0$, and also $-1 \leq \cos(\hat{a}_{n_T}(t)t - \theta) \leq 1$. Using inequalities (20) and (A6) in Eq. (A7), for any time t that M remains inside $S_\theta^+(t)$, the following is true:

$$-a_T(t)[1+K_2(t)\nu]/V_e \leq -a_T(t)[1+K_2(t)\nu]/V_S(t) \leq \dot{\theta}_1(t) \leq a_T(t)\left(1-K_2(t)\sqrt{\nu^2-1}\right)/V_S(t) \leq a_T(t)\left(1-K_2(t)\sqrt{\nu^2-1}\right)/V_e \tag{A8}$$

Since $a_T(t), K_2(t) > 0$, by inequality (A6), the left-hand side (LHS) of the inequality (A8) is negative at any time t. If $K_2(t) > 1/\sqrt{\nu^2-1}$ for all $t > t_0$ in inequality (A8), the right hand side (RHS) of inequality (A8) is also negative at any time $t > t_0$, which in turn implies that $\dot{\theta}_1(t) < 0$ for all time t for which $\theta(t) \in S_\theta^+(t)$. Then, if $\dot{\theta}(t) > 0$, by Lemma 6, $\dot{\theta}$ increases with t, that is, $\dot{\theta}(t) > \dot{\theta}(t_0) > 0$, for all time t that M is in the $S_\theta^+(t)$ sector. Because the sectors rotate at an angular rate $-K_2 a_{n_T}(t)/k$, which is negative as $a_T(t)$, $K_2(t)$, $k > 0$, the relative angular rate of M with respect to the sectors in the polar plane $\dot{\theta}_{\text{rel}}(t) = \dot{\theta}(t) - (-K_2 a_{n_T}(t)/k) > \dot{\theta}(t_0)$ is positive and bounded below by a positive quantity at all time t for which $\theta(t) \in S_\theta^+(t)$. Therefore, there exists a finite time $t = t_1 > t_0$ such that for any $t > t_1$,

$$\int_{t_0}^{t} \dot{\theta}_{\text{rel}}(\tau)\,\mathrm{d}\tau > \omega$$

where $\omega = (2/k)\sin^{-1}(1/\nu)$ is the angular spread of the $S_\theta^+(t)$ sector. This implies that M comes out of the $S_\theta^+(t)$ sector at some finite time $t \in (t_0, t_1]$.

On the other hand, when $a_T(t) > 0$, but $\dot{\theta}(t) < 0$ at some time $t \geq t_0$, then by Condition 3 of Theorem 2, $K_2(t) < 0$. In a similar way, the following inequality of $\dot{\theta}_1(t)$ is obtained for all time t that M remains inside $S_\theta^+(t)$:

$$-a_T(t)\left(1+K_2(t)\sqrt{\nu^2-1}\right)/V_e \leq -a_T(t)\left(1+K_2(t)\sqrt{\nu^2-1}\right)/V_S(t) \leq \dot{\theta}_1(t) \leq a_T(t)[1-K_2(t)\nu]/V_S(t) \leq a_T(t)[1-K_2(t)\nu]/V_e \tag{A9}$$

By similar argument, if $K_2(t) < -1/\sqrt{\nu^2-1}$ for all $t > t_0$ in inequality (A9), then $\dot{\theta}_1(t) > 0$ for all time t for which $\theta(t) \in S_\theta^+(t)$. This in turn implies that, for $\dot{\theta}(t) < 0$, by Lemma 6, $\dot{\theta}$ decreases with t, that is, $\dot{\theta}(t) < \dot{\theta}(t_0) < 0$, for all time in the $S_\theta^+(t)$ sector. Also, the angular rate of the sectors in the polar plane is $-K_2 a_{n_T}(t)/k$, which is positive. These lead to a nonzero and negative relative angular rate ($\dot{\theta}_{\text{rel}}(t)$) of M, which is bounded above by a negative quantity, for all time t for which $\theta(t) \in S_\theta^+(t)$. Hence, following a similar argument, it can be shown that M comes out of the $S_\theta^+(t)$ sector at some finite time $t > t_0$.

Next, consider $a_T(t) > 0$, but $\dot{\theta}(t) = 0$ at time $t = t_0$. Then, by Eq. (18), $\dot{\theta}(t) \neq 0$ for $t = t_0 + \varepsilon$ for arbitrarily small $\varepsilon > 0$. Thus, by the previous argument, if Conditions 3 and 4 of this theorem hold for all $t > t_0$, M would come out of the $S_\theta^+(t)$ sector at some finite time $t > t_0$.

Similar results can be proved in the same way for $a_T(t) \leq 0$ at some time $t \geq t_0$, for which M remains inside $S_\theta^+(t)$. Therefore, if $M_0(r_0, \theta_0) \in S_\theta^+(t_0)$ and $|K_1| = |\nu K_2| > 1/\sqrt{1-1/\nu^2}$ and $\text{sgn}(K_1(t)) = \text{sgn}(a_T\dot{\theta}(t))$, apart from Conditions 1 and 2 of the theorem, for all time t during the engagement, then M first comes out of $S_\theta^+(t)$ sector in the polar plane at some finite time $t = t_2 > t_0$ and finally reaches the origin T, that is, the interceptor intercepts the target at some finite time $t = t_3 > t_2 > t_0$, as ensured by Theorem 1. □

A5 Proof of Theorem 3

From Lemma 4 and Theorem 1, it is evident that, if the conditions $\nu > \sqrt{2}$ and $N > 2 + 2/\sqrt{\nu^2-1} > 1 + 1/\nu$ are satisfied, then as M lies in $S_\theta^-(t)$ sector in the polar plane at some time $t = t_1$, it will ultimately reach the target in some finite time $t = t_2 > t_1$ if $\text{sgn}(K_1) = \text{sgn}(a_T\dot{\theta}(t))$ for all time $t > t_1$ during the engagement. From Eqs. (18) and (19),

$$R\ddot{\theta}(t) = [-2\dot{\theta}(t) + a_{n_T}(t)]V_T\cos(\hat{a}_{n_T}(t)t - \theta(t)) - [(N-2)\dot{\theta}(t) + K_2 a_{n_T}(t)]V_M\cos(k\theta(t) + \gamma_{n_T}(t)t + \phi_0) \tag{A10}$$

From inequality (12), for $\theta(t) \in S_\theta^-(t)$, $|\sin(k\theta + K_2 a_{n_T}(t)t + \phi_0)| \leq 1/\nu$. Since $\nu > \sqrt{2}$ is considered and $S_\theta^-(t) \subset \sigma_R^-(t)$, as shown in Fig. 4, from Eq. (9), $\cos(k\theta + \gamma_{n_T}(t)t + \phi_0) > 0$ for $v_R(\theta, t) < 0$. Hence,

$$\cos(k\theta + \gamma_{n_T}(t)t + \phi_0) \geq \sqrt{\nu^2-1}/\nu \tag{A11}$$

$$-1 \leq \cos(\hat{a}_{n_T}(t)t - \theta) \leq 1 \tag{A12}$$

Consider $a_T(t_3) > 0$, $\dot{\theta}(t_3) > 0$, where $t_3 \in [t_1, t_2)$. Here, $\text{sgn}(K_1(t_3)) = \text{sgn}(a_T\dot{\theta}(t_3)) \Rightarrow K_2(t_3) > 0$. Also, $N > 2 + 2/\sqrt{\nu^2-1} > 2$ by the theorem. First, consider $\dot{\theta}(t_3) > a_{n_T}(t_3)/2 > 0 \Rightarrow \dot{\theta}(t_3) > -K_2 a_{n_T}(t_3)/(N-2)$. Using inequalities (A11) and (A12) in Eq. (A10) for time $t = t_3$,

$$(-2\dot{\theta} + a_{n_T})V_T - [(N-2)\dot{\theta} + K_2 a_{n_T}]V_M \leq R\ddot{\theta} \leq -\left([-2\dot{\theta} + a_{n_T}] - [(N-2)\dot{\theta} + K_2 a_{n_T}]\sqrt{\nu^2-1}\right)V_T \tag{A13}$$

The LHS of inequality (A13) as well as the RHS of inequality (A13) are negative since $K_2(t_3) > 0$ and $N > 2(1 + 1/\sqrt{\nu^2-1})$, which ensures that $\dot{\theta}(t)$ decreases with time at time $t = t_3$.

Next, consider $0 < \dot{\theta}(t_3) \leq a_{n_T}(t_3)/2 \Rightarrow \dot{\theta}(t_3) > -K_2 a_{n_T}(t_3)/(N-2)$. In a similar way, the inequality of $\ddot{\theta}$ is obtained for time $t = t_3$ as

$$-(-2\dot{\theta} + a_{n_T})V_T - [(N-2)\dot{\theta} + K_2 a_{n_T}]V_M \leq R\ddot{\theta} \leq \left([-2\dot{\theta} + a_{n_T}] - [(N-2)\dot{\theta} + K_2 a_{n_T}]\sqrt{\nu^2-1}\right)V_T \tag{A14}$$

The LHS of inequality (A14) is negative, whereas, the RHS of inequality (A14) is negative if $K_2(t_3) > 1/\sqrt{\nu^2-1}$ and

$N > 2(1 + 1/\sqrt{\nu^2 - 1})$. Therefore, for $a_T(t_3) > 0$, $\dot{\theta}(t_3) > 0$, where $t = t_3 \in [t_1, t_2)$, $K_2(t) > 1/\sqrt{\nu^2 - 1}$ ensures that $\dot{\theta}(t)$ decreases with time at time $t = t_3$. Following similar methodology, it can be shown that, for $a_T(t_3) > 0$ and $\dot{\theta}(t_3) < 0$, where $t = t_3 \in [t_1, t_2)$, $N > 2(1 + 1/\sqrt{\nu^2 - 1})$ and $K_2(t) < -1/\sqrt{\nu^2 - 1}$ ensures that $\theta(t)$ increases with time at time $t = t_3$.

Similar results can be proved for $a_T(t) < 0$ in the same way. Thus, if the conditions, mentioned in the theorem, that is, $\nu > \sqrt{2}$, $N > 2 + 2/\sqrt{\nu^2 - 1} > 1 + 1/\nu$, $\text{sgn}(K_1(t)) = \text{sgn}(a_T\dot{\theta}(t))$, and $|K_1(t)| > 1/\sqrt{1 - 1/\nu^2}$ are satisfied, then in the $S_\theta^-(t)$ sector at any time t, if $|\dot{\theta}(t)| > 0$, then $\text{sgn}(\ddot{\theta}(t)) = -\text{sgn}(\dot{\theta}(t))$. This along with the continuity of $\dot{\theta}(t)$ in time t ensures that $|\dot{\theta}(t)|$ decreases with time for all subsequent time t until $|\dot{\theta}(t)| = 0$ at some finite time $t = t_4 > t_3$.

If $v_\theta(\theta, t) > 0 (< 0)$ for all $t \in [t_3, t_4)$, then at $t = t_4 + \varepsilon$ for an arbitrarily small $\varepsilon > 0$, $v_\theta(\theta, t) < 0 (> 0)$. Following similar arguments, if the conditions on ν, N, and K_1 hold for all time $t > t_4$, $|\dot{\theta}|$ again decreases to zero at some finite time. This process continues until interception, that is, after $\dot{\theta}$ reaches zero once, then onward $\dot{\theta}$ chatters about zero until M reaches the origin T in the polar plane. □

A6 Proof of Corollary 2

From Theorems 1 and 2, for successful interception of the piecewise continuously maneuvering target from any initial engagement geometry, the required APPN guidance law in Eq. (6) can be written as

$$a_M = NV_M\dot{\theta} + K_1 a_T = NV_M\dot{\theta} + |K_1|a_T\text{sgn}(K_1) = NV_M|\dot{\theta}|\text{sgn}(\dot{\theta}) + |K_1|a_T\text{sgn}(a_T\dot{\theta}) = (NV_M|\dot{\theta}| + |K_1 a_T|)\text{sgn}(\dot{\theta}) \quad \text{(A15)}$$

where $N > 2 + 2/\sqrt{\nu^2 - 1} > 1 + 1/\nu$ and $|K_1| > \sqrt{1 - 1/\nu^2}$, which implies that $|K_1 a_T(t)| > \sqrt{1 - 1/\nu^2}a_T(t)$ for all time t. Hence, at any time t, a threshold magnitude of a_M, given as $C_{1_t} = (2 + 2/\sqrt{\nu^2 - 1})V_M|\dot{\theta}| + \sqrt{1 - 1/\nu^2}a_{T_{\max}}$, is obtained such that $|a_M(t)| > C_{1_t}$ for all time t is sufficient, by Theorems 1 and 2, to ensure interception from any initial engagement geometry in a finite time.

If the target maneuver capability is known a priori and the navigation gain $N = 2 + 2/\sqrt{\nu^2 - 1} > 1 + 1/\nu$ is considered, then at any time t during the engagement,

$$a_M(t) = (NV_M|\dot{\theta}(t)| + C_2)\text{sgn}(\dot{\theta}(t)) = C_1(t)\text{sgn}(\dot{\theta}(t)) \quad \text{(A16)}$$

where the bias term $C_2 = a_{T_{\max}}\sqrt{1 - 1/\nu^2}$ is a constant, implies that $C_1(t) > C_{1_t}$. Also, note that the interceptor lateral acceleration command, given by Eq. (A16), satisfies the conditions of Theorem 3, which ensures finite demand of interceptor lateral acceleration at the endgame of engagement. □

References

[1] Nesline, F. W., and Zarchan, P., "New Look at Classical vs Modern Homing Missile Guidance," *Journal of Guidance, Control, and Dynamics*, Vol. 4, No. 1, 1981, pp. 78–85. doi:10.2514/3.56054

[2] Yuan, C. L., "Homing and Navigational Courses of Automatic Target-Seeking Devices," *Journal of Applied Physics*, Vol. 19, No. 12, Dec. 1948, pp. 1122–1128. doi:10.1063/1.1715028

[3] Murtaugh, S. A., and Criel, H. E., "Fundamentals of Proportional Navigation," *IEEE Spectrum*, Vol. 3, No. 6, Dec. 1966, pp. 75–85.

[4] Guelman, M., "A Qualitative Study of Proportional Navigation," *IEEE Transactions on Aerospace and Electronic Systems*, Vol. 7, No. 4, July 1971, pp. 637–643.

[5] Guelman, M., "The Closed-Form Solution of True Proportional Navigation," *IEEE Transactions on Aerospace and Electronic Systems*, Vol. 12, No. 4, July 1976, pp. 472–482.

[6] Becker, K., "Closed Form Solution of Pure Proportional Navigation," *IEEE Transactions on Aerospace and Electronic Systems*, Vol. 26, No. 3, April 1990, pp. 526–533. doi:10.1109/7.106131

[7] Yuan, P. J., and Chern, J. S., "Solutions of True Proportional Navigation for Maneuvering and Nonmaneuvering Targets," *Journal of Guidance, Control, and Dynamics*, Vol. 15, No. 1, Jan.–Feb. 1992, pp. 268–271.

[8] Dhar, A., and Ghose, D., "Capture Region for a Realistic TPN Guidance Law," *IEEE Transactions on Aerospace and Electronic Systems*, Vol. 29, No. 3, July 1993, pp. 995–1003. doi:10.1109/7.220946

[9] Ghose, D., "On the Generalization of True Proportional Navigation," *IEEE Transactions on Aerospace and Electronic Systems*, Vol. 30, No. 2, April 1994, pp. 545–555. doi:10.1109/7.272277

[10] Shukla, U. S., and Mahapatra, P. R., "The Proportional Navigation Dilemma—Pure or True," *IEEE Transactions on Aerospace and Electronic Systems*, Vol. 26, No. 2, March 1990, pp. 382–392. doi:10.1109/7.53445

[11] Yang, C. D., and Yang, C. C., "A Unified Approach to Proportional Navigation," *IEEE Transactions on Aerospace and Electronic Systems*, Vol. 33, No. 2, April 1997, pp. 557–567.

[12] Tyan, F., "Unified Approach to Missile Guidance Laws: A 3D Extension," *IEEE Transactions on Aerospace and Electronic Systems*, Vol. 41, No. 4, Oct. 2005, pp. 1178–1199.

[13] Bryson, A. E., and Ho, Y.-C., *Applied Optimal Control — Optimization, Estimation and Control*, Taylor and Francis, New York, 1975, pp. 154–155.

[14] Zarchan, P., *Tactical and Strategic Missile Guidance*, Vol. 124, Progress in Astronautics and Aeronautics, AIAA, Washington, DC, 1990, pp. 11–29, 143–152.

[15] Siouris, G. M., *Missile Guidance and Control Systems*, Springer–Verlag, New York, 2004, pp. 194–227.

[16] Guelman, M., "Proportional Navigation with a Maneuvering Target," *IEEE Transactions on Aerospace and Electronic Systems*, Vol. 8, No. 3, May 1972, pp. 364–371.

[17] Guelman, M., "Missile Acceleration in Proportional Navigation," *IEEE Transactions on Aerospace and Electronic Systems*, Vol. 9, No. 3, May 1973, pp. 462–463.

[18] Ghawghawe, S. N., and Ghose, D., "Pure Proportional Navigation Against Time-Varying Target Maneuvers," *IEEE Transactions on Aerospace and Electronic Systems*, Vol. 32, No. 4, Oct. 1996, pp. 1336–1347. doi:10.1109/7.543854

[19] Ghose, D., "True Proportional Navigation With Maneuvering Target," *IEEE Transactions on Aerospace and Electronic Systems*, Vol. 30, No. 1, Jan. 1994, pp. 229–237. doi:10.1109/7.250423

[20] Garber, V., "Optimum Intercept Laws for Accelerating Targets," *AIAA Journal*, Vol. 6, No. 11, 1968, pp. 2196–2198. doi:10.2514/3.4962

[21] Siouris, G. M., "Comparison Between Proportional and Augmented Proportional Navigation," *Nachrichtentechnische Zeitschrift*, Vol. 27, No. 7, July 1974, pp. 278–280.

[22] Lin, C. F., *Modern Navigation, Guidance and Control Processing*, Vol. 2, Prentice–Hall, Upper Saddle River, NJ, 1991, pp. 474–477.

[23] Babu, K. R., Sarma, I. G., and Swamy, K. N., "Switched Bias Proportional Navigation for Homing Guidance Against Highly Maneuvering Targets," *Journal of Guidance, Control, and Dynamics*, Vol. 17, No. 6, 1994, pp. 1357–1363. doi:10.2514/3.21356

[24] Kim, Y., and Seo, J. H., "The Realization of the Three Dimensional Guidance Law Using Modified Augmented Proportional Navigation," *Proceedings of Conference on Decision and Control and European Control Conference*, IEEE, Piscataway, NJ, Dec. 1996, pp. 2707–2712.

[25] Talole, S. E., and Banavar, R. N., "Proportional Navigation Through Predictive Control," *Journal of Guidance, Control, and Dynamics*, Vol. 21, No. 6, 1998, pp. 1004–1006. doi:10.2514/2.4339

[26] Cloutier, J. R., "Adaptive Matched Augmented Proportional Navigation," U.S. Patent No. US H1980 H, Aug. 2001.

[27] Speyer, J. L., Kim, K. D., and Tahk, M. J., "Passive Homing Missile Guidance Law Based on New Target Maneuver Models," *Journal of Guidance, Control, and Dynamics*, Vol. 13, No. 5, 1990, pp. 803–812. doi:10.2514/3.25405

[28] Shinar, J., and Shima, T., "Nonorthodox Guidance Law Development Approach for Intercepting Maneuvering Targets," *Journal of Guidance, Control, and Dynamics*, Vol. 25, No. 4, 2002, pp. 658–666. doi:10.2514/2.4960

[29] Ariff, O., Zbikowski, R., Tsourdos, A., and White, B. A., "Differential Geometric Guidance Based on the Involute of the Target's Trajectory," *Journal of Guidance, Control, and Dynamics*, Vol. 28, No. 5, 2005, pp. 990–996.
doi:10.2514/1.11041

[30] White, B. A., Zbikowski, R., and Tsourdos, A., "Direct Intercept Guidance using Differential Geometry Concepts," *IEEE Transactions on Aerospace and Electronic Systems*, Vol. 43, No. 3, 2007, pp. 899–919.
doi:10.1109/TAES.2007.4383582

[31] Moosapour, S. S., Alizadeh, G., Khanmohammadi, S., and Moosapour, S. H., "A Novel Nonlinear Robust Guidance Law Design Based on SDRE Technique," *International Journal of Aeronautical and Space Sciences*, Vol. 13, No. 3, Sept. 2012, pp. 369–376.

[32] Vathsal, S., and Sarkar, A. K., "Current Trends in Tactical Missile Guidance," *Defence Science Journal*, Vol. 55, No. 3, July 2005, pp. 265–280.

[33] Ghosh, S., Ghose, D., and Raha, S., "Capturability of Augmented Proportional Navigation (APN) Guidance with Nonlinear Engagement Dynamics," *Proceedings of American Control Conference*, IEEE, Piscataway, NJ, June 2013, pp. 1–6.

[34] Rudin, W., *Principles of Mathematical Analysis*, McGraw–Hill, New York, 1976, pp. 83–95, 322–324.

[35] Athreya, K. B., and Lahiri, S., *Measure Theory*, Hindustan Books, New Delhi, India, 2006, pp. 48–61.

[36] Fossier, M. W., "Development of Radar Homing Missiles," *Journal of Guidance, Control, and Dynamics*, Vol. 7, No. 6, 1984, pp. 641–651.
doi:10.2514/3.19908

[37] Flanders, H., "Differentiation Under the Integral Sign," *The American Mathematical Monthly*, Vol. 80, No. 6, 1973, pp. 615–627.
doi:10.2307/2319163

This article has been cited by:

1. Wenxue Chen, Yudong Hu, Changsheng Gao, Wuxing Jing. 2024. Luring cooperative capture guidance strategy for the pursuit—evasion game under incomplete target information. *Astrodynamics* **8**:4, 675-688. [Crossref]
2. Ang Huang, Jianglong Yu, Yumeng Liu, Yongzhao Hua, Xiwang Dong, Zhang Ren. 2024. Multitask-constrained reentry trajectory planning for hypersonic gliding vehicle. *Aerospace Science and Technology* **155**, 109636. [Crossref]
3. Cheol-Goo Jung, Chang-Hun Lee. 2024. Optimal Impact Angle Control Guidance Law Considering Aerodynamic Drag. *Journal of Guidance, Control, and Dynamics* **47**:11, 2435-2443. [Citation] [Full Text] [PDF] [PDF Plus]
4. Haowen Luo, Shaoming He. 2024. Small-Data-Driven Multitask Computational Guidance for Constrained Impact. *Journal of Aerospace Information Systems* **21**:10, 828-845. [Abstract] [Full Text] [PDF] [PDF Plus]
5. Wenxue CHEN, Yudong HU, Changsheng GAO, Ruoming AN. 2024. Three-dimensional multi-constraint analytical capture zone against maneuvering targets with velocity advantages. *Chinese Journal of Aeronautics* **118**. . [Crossref]
6. Jianfeng Li, Cheng Xu, Shenmin Song. Three-Dimensional Guidance Law Design against Maneuvering Target via Deep Reinforcement Learning 3773-3778. [Crossref]
7. Axing Xi, Yuanli Cai, Yifan Deng, Haonan Jiang. A Suboptimal Interception Guidance Law Based on Event-Triggered Mechanism 366-371. [Crossref]
8. Peng Sun, Siqi Li, Bing Zhu, Zewei Zheng, Zongyu Zuo. 2024. Vision-based finite-time prescribed performance control for uncooperative UAV target-tracking subject to field of view constraints. *ISA Transactions* **149**, 168-177. [Crossref]
9. Nobin Paul, Debasish Ghose. Qualitative Analysis of Variable Speed Proportional Navigation Guidance Law . [Abstract] [PDF] [PDF Plus]
10. Xiaoqi Qiu, Peng Lai, Changsheng Gao, Wuxing Jing. 2024. Recorded recurrent deep reinforcement learning guidance laws for intercepting endoatmospheric maneuvering missiles. *Defence Technology* **31**, 457-470. [Crossref]
11. Peng Sun, Bing Zhu, Siqi Li. 2024. Vision-Based Prescribed Performance Control for UAV Target Tracking Subject to Actuator Saturation. *IEEE Transactions on Intelligent Vehicles* **9**:1, 2382-2389. [Crossref]
12. Yuting Lu, Yang Yu, Qilun Zhao, Tuo Han, Qinglei Hu, Dongyu Li. Capturability of the Pulsed Guidance Law Based on Differential Game Theory 7125-7130. [Crossref]
13. A-xing Xi, Yuan-li Cai, Yi-fan Deng, Hao-nan Jiang. 2023. Zero-sum differential game guidance law for missile interception engagement via neuro-dynamic programming. *Proceedings of the Institution of Mechanical Engineers, Part G: Journal of Aerospace Engineering* **237**:14, 3352-3366. [Crossref]
14. Shaobo WANG, Yang GUO, Shicheng WANG, Lixin WANG, Yanhua TAO, Zhengfei PENG. 2023. Capurability analysis for arbitrarily high-speed maneuvering targets. *Chinese Journal of Aeronautics* **36**:10, 375-390. [Crossref]
15. Hongyan Li, Hong Tao, Jiang Wang, Shaoming He. 2023. Three-Dimensional Optimal Homing Guidance Without Terminal Maneuverability Advantage. *Journal of Guidance, Control, and Dynamics* **46**:9, 1774-1784. [Abstract] [Full Text] [PDF] [PDF Plus]
16. Brian Gaudet, Roberto Furfaro. Line of Sight Curvature for Missile Guidance using Reinforcement Meta-Learning . [Abstract] [PDF] [PDF Plus]
17. V. S. Shincy, Satadal Ghosh. 2023. Sliding-Mode-Control–Based Instantaneously Optimal Guidance for Precision Soft Landing on Asteroid. *Journal of Spacecraft and Rockets* **60**:1, 146-159. [Abstract] [Full Text] [PDF] [PDF Plus]
18. Liu Jiaqi, Chen Bailin, Yang Wenlong, Shi Zhongjiao, Wang Wei. Tracking Differentiation Guidance Law Based on Backstepping Control 5054-5062. [Crossref]
19. Chunhua Cheng, Mingming Huo, Dongsheng Hao, SiMin Bi. Guidance Law Design Against Unknown Maneuvering Target Based on Two ESOs 380-391. [Crossref]
20. Xin Sun, Hui Wang, Kaiyang Guo, Yuru Bin, Heting Wang, Keqing Guo. 2023. Analysis of Line-of-Sight Angle Characteristics for Intercepting a Non-Maneuvering Target With Impact Angle Constraints. *IEEE Access* **11**, 41565-41577. [Crossref]
21. Suryadeep Nath, Debasish Ghose. 2022. A two-phase evasive strategy for a pursuit-evasion problem involving two non-holonomic agents with incomplete information. *European Journal of Control* **68**, 100677. [Crossref]
22. Yiting Tan, Wuxing Jing, Changsheng Gao, Ruoming An. 2022. Adaptive improved super-twisting integral sliding mode guidance law against maneuvering target with terminal angle constraint. *Aerospace Science and Technology* **129**, 107820. [Crossref]

23. Axing Xi, Yuanli Cai. 2022. A Nonlinear Finite-Time Robust Differential Game Guidance Law. *Sensors* **22**:17, 6650. [Crossref]
24. Kebo LI, Zhihui BAI, Hyo-Sang SHIN, Antonios TSOURDOS, Min-Jea TAHK. 2022. Capturability of 3D RTPN guidance law against true-arbitrarily maneuvering target with maneuverability limitation. *Chinese Journal of Aeronautics* **35**:7, 75-90. [Crossref]
25. Hong Tao, Defu Lin, Shaoming He, Tao Song, Ren Jin. 2022. Optimal terminal-velocity-control guidance for intercepting non-cooperative maneuvering quadcopter. *Journal of Field Robotics* **39**:4, 457-472. [Crossref]
26. Nobin Paul, Debasish Ghose. Longitudinal acceleration-based guidance law inspired from hawk's attack against a maneuvering target . [Abstract] [PDF] [PDF Plus]
27. Ke-Bo Li, Zhi-Hui Bai, Hyo-Sang Shin, Antonios Tsourdos, Min-Jea Tahk. Capturability of 3D RTPN Against True-Arbitrarily Maneuvering Target with Maneuverability Limitation 4511-4528. [Crossref]
28. Xiuxia Yang, Zijie Jiang, Yi Zhang, Hao Yu, Chenlei Wang. Dynamic Programming Guidance Law for Maneuvering Target 2413-2426. [Crossref]
29. Chang Yu, Bing Zhu, Zongyu Zuo. 2021. Three-Dimensional Optimal Guidance with Lyapunov Redesign for UAV Interception. *Guidance, Navigation and Control* **01**:04. . [Crossref]
30. Yi Mao, Zhijie Chen, Yi Yang, Yuxin Hu. 2021. A novel adaptive heuristic dynamic programming-based algorithm for aircraft confrontation games. *Fundamental Research* **1**:6, 792-799. [Crossref]
31. Suwon Lee, Youngjun Lee, Seokwon Lee, Youdan Kim, Yongsu Han, Jangseong Park. 2021. Data-Driven Capturability Analysis for Pure Proportional Navigation Guidance Considering Target Maneuver. *International Journal of Aeronautical and Space Sciences* **22**:5, 1209-1221. [Crossref]
32. Fei Liao, Sheng Zhang. 2021. Modified three-dimensional true proportional navigation and its inverse optimal form. *Optimal Control Applications and Methods* **42**:5, 1441-1466. [Crossref]
33. Diganta Bhattacharjee, Animesh Chakravarthy, Kamesh Subbarao. 2021. Nonlinear Model Predictive Control and Collision-Cone-Based Missile Guidance Algorithm. *Journal of Guidance, Control, and Dynamics* **44**:8, 1481-1497. [Abstract] [Full Text] [PDF] [PDF Plus]
34. Peng Sun, Bing Zhu, Zongyu Zuo, Michael V. Basin. 2021. Vision-based finite-time uncooperative target tracking for UAV subject to actuator saturation. *Automatica* **130**, 109708. [Crossref]
35. A. Sadik Satir, Umut Demir, Gulay Goktas Sever, N. Kemal Ure. Nonlinear Model Based Guidance with Deep Learning Based Target Trajectory Prediction Against Aerial Agile Attack Patterns 2607-2612. [Crossref]
36. Shincy V S, Satadal Ghosh. A Novel Sliding Mode-based Guidance for Soft Landing of a Spacecraft on an Asteroid . [Abstract] [PDF] [PDF Plus]
37. Mehmet Ugur Akcal, Girish Chowdhary. A Predictive Guidance Scheme for Pursuit-Evasion Engagements . [Abstract] [PDF] [PDF Plus]
38. Diganta Bhattacharjee, Kamesh Subbarao, Animesh Chakravarthy. Set-Membership Filtering-Based Pure Proportional Navigation . [Abstract] [PDF] [PDF Plus]
39. Kumar R. Dinkar, Satadal Ghosh. Indicator Probabilistic Acceleration Velocity Obstacles for Dynamic Collision Avoidance in Uncertain Environments . [Abstract] [PDF] [PDF Plus]
40. Suwon Lee, Youdan Kim. 2020. Vector-Field-Based Guidance for Exoatmospheric Target Interception. *IEEE Transactions on Aerospace and Electronic Systems* **56**:6, 4353-4366. [Crossref]
41. Manikandan L.P, Satadal Ghosh. Online Hybrid Motion Planning for Unmanned Aerial Vehicles in Planar Environments 1533-1540. [Crossref]
42. Haoxiang Chen, Jie Wu, Fanhong Meng, Qunhua Pan, Ying Nan. Trajectory Optimization of Multi-Aircraft Confrontation Based on Improved Natural Computation 1262-1266. [Crossref]
43. Diganta Bhattacharjee, Animesh Chakravarthy, Kamesh Subbarao. Nonlinear Model Predictive Control based Missile Guidance for Target Interception . [Abstract] [PDF] [PDF Plus]
44. Xi Wang, Guanzheng Tan, Yusi Dai, Fanlei Lu, Jian Zhao. 2020. An Optimal Guidance Strategy for Moving-Target Interception by a Multirotor Unmanned Aerial Vehicle Swarm. *IEEE Access* **8**, 121650-121664. [Crossref]
45. Guangyan Xu, Kun Sun, Hao Liu. Optimal control of missile interception process based on adaptive dynamic programming 1256-1260. [Crossref]

46. Amit Kumar, Aparajita Ojha. 2019. Experimental Evaluation of Certain Pursuit and Evasion Schemes for Wheeled Mobile Robots. *International Journal of Automation and Computing* **16**:4, 491-510. [Crossref]
47. Jingliang Sun, Chunsheng Liu, Jiao Dai. Robust optimal control for missile-target guidance systems via adaptive dynamic programming 836-841. [Crossref]
48. Huaji WANG, Dayuan ZHANG, Tao ZHANG, Humin LEI, Yexing WANG, Pengfei Zhang. Capturability Analysis of Pure Proportional Navigation Guidance Law for Intercepting Hypersonic Targets 1-7. [Crossref]
49. Danyao Zhang, Qingyu Du, Yijia Xie, Jianzhong Qiao. A New Composite Proportional Navigation Entry Guidance Strategy for Glider Under Multiple Uncertainties 531-536. [Crossref]
50. Suwon Lee, Seokwon Lee, Sungjun Ann, Jaeho Lee, Youdan Kim. Vector Field Based Guidance Law for Intercepting Maneuvering Target 223-228. [Crossref]
51. Bing Zhu, Lihua Xie, Chun Yin. Dynamic mission allocation for interceptions by using multiple rotary-wing UAVs 441-446. [Crossref]
52. Bing Zhu, Abdul Hanif Bin Zaini, Lihua Xie. 2017. Distributed Guidance for Interception by Using Multiple Rotary-Wing Unmanned Aerial Vehicles. *IEEE Transactions on Industrial Electronics* **64**:7, 5648-5656. [Crossref]
53. Jingliang Sun, Chunsheng Liu, Qing Ye. 2017. Robust differential game guidance laws design for uncertain interceptor-target engagement via adaptive dynamic programming. *International Journal of Control* **90**:5, 990-1004. [Crossref]
54. Lei Sun, Pu Lian, Xiaofei Chang. Capturability of Retro-Augmented Proportional Navigation Guidance Law Against Higher Speed Maneuvering Target . [Citation] [PDF] [PDF Plus]
55. Satadal Ghosh, Duane T. Davis, Timothy H. Chung. A guidance law for avoiding specific approach angles against maneuvering targets 4142-4147. [Crossref]
56. Yongwei Zhang, Min Gao, Suochang Yang, Dan Fang. 2016. An adaptive proportional navigation guidance law for guided mortar projectiles. *The Journal of Defense Modeling and Simulation: Applications, Methodology, Technology* **13**:4, 467-475. [Crossref]
57. Chethan Upendra Chithapuram, Aswani Kumar Cherukuri, Yogananda V. Jeppu. 2016. Aerial vehicle guidance based on passive machine learning technique. *International Journal of Intelligent Computing and Cybernetics* **9**:3, 255-273. [Crossref]
58. Wu Yanan, Zhang Ran, Li Huifeng. Terminal guidance with impact angle constraint based on a practical flight strategy 289-294. [Crossref]
59. Bing Zhu, Abdul Hanif Bin Zaini, Lihua Xie, Guoan Bi. Distributed guidance for interception by using multiple rotary-wing unmanned aerial vehicles 1034-1039. [Crossref]
60. Bing Zhu, Juanjuan Xu, Abdul Hanif Bin Zaini, Lihua Xie. A three-dimensional integrated guidance law for rotary UAV interception 726-731. [Crossref]
61. Gil Weiss, Ilan Rusnak. 2015. All-Aspect Three-Dimensional Guidance Law Based on Feedback Linearization. *Journal of Guidance, Control, and Dynamics* **38**:12, 2421-2428. [Abstract] [Full Text] [PDF] [PDF Plus]
62. Larasmoyo Nugroho, Ali Turker Kutay. Capturability of combined augmented proportional navigation against a pull-up maneuvering target 1-9. [Crossref]